

UNIVERSIDAD DE CONCEPCIÓN



CENTRO DE INVESTIGACIÓN EN
INGENIERÍA MATEMÁTICA (CI²MA)



A posteriori error estimates for the problem of electrostatics
with a dipole source

ANA ALONSO-RODRIGUEZ, JESSIKA CAMAÑO,
RODOLFO RODRÍGUEZ, ALBERTO VALLI

PREPRINT 2013-10

SERIE DE PRE-PUBLICACIONES

A POSTERIORI ERROR ESTIMATES FOR THE PROBLEM OF ELECTROSTATICS WITH A DIPOLE SOURCE

A. ALONSO RODRÍGUEZ, J. CAMAÑO, R. RODRÍGUEZ, AND A. VALLI

ABSTRACT. Electroencephalography is a non-invasive technique for detecting brain activity from the measurement of the electric potential on the head surface. In mathematical terms, it reduces to an inverse problem in which the goal is to determine the source that has generated the electric field from measurements of boundary values of the electric potential. Since for reasonable models the time-variation of the electric and magnetic fields can be disregarded, the mathematical modeling of the corresponding forward problem leads to an electrostatics problem with a current dipole source. This is a singular problem, since the current dipole model involves first-order derivatives of a Dirac delta measure. Its solution lies in L^p for $1 \leq p < 3/2$ in three dimensional domains and $1 \leq p < 2$ in the two dimensional case.

We consider the numerical approximation of the forward problem by means of standard piecewise linear continuous finite elements. We prove a priori error estimates in L^p norm. Then, we propose a residual-type a posteriori error estimator. We prove that it is reliable and efficient; namely, it yields global upper and local lower bounds for the corresponding norms of the error. Finally, we use this estimator to guide an adaptive procedure, which is experimentally shown to lead to an optimal order of convergence.

1. INTRODUCTION

Electroencephalography (EEG) is a widely used technique for reconstruction of brain activity. The task is to estimate the cerebral current sources underlying a measured distribution of the scalp electric potential. The inverse problem requires a model for the forward problem, i.e., the computation of the scalp potential given a neural current source. Since the frequency spectrum for electrophysiological signal is frequently between 0.1 and 100 Hz, most works on biomedical applications focus on the static approximation of Maxwell equations. Concerning the source, the activity measured in EEG is the result of movement of ions that, creating an electrical potential difference, generates the so-called primary current. Since the source is localized, it is generally modeled as a current dipole centered at a point \mathbf{x}_0 with moment \mathbf{p} .

For computing the solution of the forward problem, the finite element method has become popular because it allows a realistic representation of the geometry and conductivity of the different tissues. In particular it allows to deal with anisotropic conductivities. In this case the forward problem is non-standard and it is usually

2010 *Mathematics Subject Classification.* Primary 65N15, 65N30, 65N50.

Key words and phrases. Residual based error estimator, dipole source, electrostatic, finite elements L^p -error, electroencephalography.

The second author was partially supported by a CONICYT and Becas Chile (Chile).

The third author was partially supported by BASAL project, CMM, Universidad de Chile and Anillo ANANUM, ACT1118, CONICYT (Chile).

solved by the subtraction approach (see [2], [18], [10]). Recently the well-posedness of the problem was studied in [16] using the duality method. There it is proved that, in the three dimensional (3D) case, the solution belongs to L^p for $1 \leq p < 3/2$. The same arguments allow proving that in the two dimensional case (2D) the solution belongs to L^p for $1 \leq p < 2$. Finite elements have been used in practice for both approaches: the subtraction method and the direct one. For the former, a sound mathematical and numerical analysis can be found in [18] under the assumption that there is a neighborhood of the source position \mathbf{x}_0 with constant conductivity. On the other hand, the direct approach is widely used in source reconstruction (see e.g. [19], [4], [17], [14]) and can be used even for a variable conductivity (smooth in a neighborhood of \mathbf{x}_0). However it has not been rigorously analyzed yet. The aim of this paper is to take advantage of the method in [16] to provide such analysis.

In spite of the fact that the solution is only in L^p , it can be approximated by standard finite elements. Specifically we use piecewise linear continuous elements on polyhedral or polygonal domains. Even though the original problem is three dimensional we present the results in more detail in the 2D framework. Under the assumption that the computational domain Ω is bounded, convex and polygonal, we develop a priori and a posteriori error analyses in L^p norm for this problem. In particular, we prove an a priori error estimate under the assumption that the meshes are quasiuniform. Since the solution is highly singular at \mathbf{x}_0 , quasiuniformity is an excessively restrictive assumption in practice. This is the reason why we also derive an a posteriori error analysis which does not need the quasiuniformity assumption. We introduce a posteriori error indicators and prove their reliability and efficiency. Subsequently, we briefly discuss the 3D case and present similar results under more stringent assumptions on the geometry of the domain and the electric conductivity. We use these error indicators to guide an adaptive scheme, which experimentally exhibits optimal order of convergence.

The paper is organized as follows. In Section 2 we state the model problem, a finite element discretization (in 2D and 3D), and give an a priori estimate of the error in L^p norm for the 2D case. In Section 3, we introduce some generalized bubble functions and prove some technical lemmas, which will be used in the sequel. The main result is presented in Section 4, where we perform the a posteriori error analysis for the 2D case. In Section 5, we briefly analyze the a priori and a posteriori estimates in 3D. Finally, in Section 6, we report some numerical results illustrating the performance of the adaptive scheme.

2. MODEL PROBLEM

In this section we introduce the model problem, propose a variational formulation and recall the existence and uniqueness of solution. Then, we consider a finite element discretization and give an a priori error estimate.

2.1. Continuous problem. We start introducing the Maxwell equations:

$$\begin{cases} \operatorname{curl} \mathbf{H} - \epsilon \frac{\partial \mathbf{E}}{\partial t} = \sigma \mathbf{E} + \mathbf{J}_p, \\ \operatorname{curl} \mathbf{E} + \mu \frac{\partial \mathbf{H}}{\partial t} = \mathbf{0}, \end{cases}$$

where \mathbf{E} and \mathbf{H} are the electric and magnetic fields, respectively, \mathbf{J}_p is the source current density, ϵ the electric permittivity, $\boldsymbol{\mu}$ the magnetic permeability and $\boldsymbol{\sigma}$ the electric conductivity.

By disregarding the time variation one obtains the static model:

$$\begin{cases} \mathbf{curl} \mathbf{H} = \boldsymbol{\sigma} \mathbf{E} + \mathbf{J}_p, \\ \mathbf{curl} \mathbf{E} = \mathbf{0}. \end{cases}$$

If we consider a simply connected domain $D \subset \mathbb{R}^3$, then there exists a scalar potential u such that $\mathbf{E} = -\nabla u$ in D . As a consequence, calculating the divergence of the first equation, we obtain

$$\operatorname{div}(\boldsymbol{\sigma} \nabla u) = \operatorname{div} \mathbf{J}_p \quad \text{in } D.$$

If Ω is a conductive domain completely included in D and $D \setminus \bar{\Omega}$ is not conductive, then, due to the properties of the div operator, the equation above is equivalent to $\operatorname{div}(\boldsymbol{\sigma} \nabla u - \mathbf{J}_p)|_{\Omega} = 0$ in Ω , $\operatorname{div}(\boldsymbol{\sigma} \nabla u - \mathbf{J}_p)|_{D \setminus \bar{\Omega}} = 0$ and $(\boldsymbol{\sigma} \nabla u - \mathbf{J}_p)|_{\Omega} \cdot \mathbf{n} = (\boldsymbol{\sigma} \nabla u - \mathbf{J}_p)|_{D \setminus \bar{\Omega}} \cdot \mathbf{n}$ on the interface $\partial\Omega$, being \mathbf{n} the outer unit normal vector to $\partial\Omega$. Since $\boldsymbol{\sigma}$ vanishes outside $\bar{\Omega}$ and \mathbf{J}_p is assumed to be supported in Ω , the electrostatics problem reads

$$\begin{cases} \operatorname{div}(\boldsymbol{\sigma} \nabla u) = \operatorname{div} \mathbf{J}_p & \text{in } \Omega, \\ (\boldsymbol{\sigma} \nabla u) \cdot \mathbf{n} = 0 & \text{on } \partial\Omega. \end{cases}$$

This is the model more frequently used for the electrical brain activity (see e.g. [13], [9], [11]).

Let us assume that a small activated region is centered at a point \mathbf{x}_0 and that the observation point is far from it. In this case the primary current \mathbf{J}_p is typically modeled as a dipole. So, in the following, we consider the electrostatic problem with a dipole as source term and homogeneous Neumann boundary condition:

$$(2.1) \quad \begin{cases} \operatorname{div}(\boldsymbol{\sigma} \nabla u) = \operatorname{div}(\mathbf{p} \delta_{\mathbf{x}_0}) & \text{in } \Omega, \\ (\boldsymbol{\sigma} \nabla u) \cdot \mathbf{n} = 0 & \text{on } \partial\Omega. \end{cases}$$

Here \mathbf{x}_0 is an inner point of Ω , and $\mathbf{p} \neq \mathbf{0}$ is the polarization vector. The conductivity $\boldsymbol{\sigma}$ is a matrix with entries in $L^\infty(\Omega)$ and uniformly positive definite, namely, there exists a positive constant σ_0 such that

$$(2.2) \quad \sum_{i,j=1}^3 \xi_i \sigma_{i,j}(\mathbf{x}) \xi_j \geq \sigma_0 \sum_{i=1}^3 \xi_i^2 \quad \forall \boldsymbol{\xi} \in \mathbb{R}^3, \quad \text{a.e. } \mathbf{x} \in \Omega.$$

Moreover we assume that there exists $r_0 > 0$ such that $\sigma_{i,j} \in W^{1,\infty}(B_{r_0}(\mathbf{x}_0))$ for $i, j = 1, 2, 3$, where $B_{r_0}(\mathbf{x}_0) := \{\mathbf{x} \in \mathbb{R}^3 : |\mathbf{x} - \mathbf{x}_0| < r_0\}$. This is a technical assumption used in [16] for the proof of the well-posedness of the problem by means of a duality argument.

Slightly modifying the arguments presented in [16], we consider the following weak formulation of (2.1): for $1 < p < 3/2$, find $u \in L^p(\Omega)$ such that

$$(2.3) \quad \begin{cases} \int_{\Omega} u \operatorname{div}(\boldsymbol{\sigma} \nabla \varphi) = -\mathbf{p} \cdot \nabla \varphi(\mathbf{x}_0) & \forall \varphi \in X_q, \\ \int_{\Omega} u = 0, \end{cases}$$

where

$$X_q := \{\varphi \in H^1(\Omega) : \varphi \in C^1(B_{r_*}(\mathbf{x}_0)), \operatorname{div}(\boldsymbol{\sigma} \nabla \varphi) \in L^q(\Omega), (\boldsymbol{\sigma} \nabla \varphi) \cdot \mathbf{n} = 0 \text{ on } \partial\Omega\},$$

being r^* a fixed number such that $0 < r^* < r_0$. Moreover, here and thereafter $\frac{1}{p} + \frac{1}{q} = 1$.

The second condition of (2.3) filters out additive constants and therefore is suitable for assuring uniqueness of the solution u .

The following theorem, which is essentially proved in [16, Remark 3.3], ensures the existence and uniqueness of solution to (2.3):

Theorem 2.1. *For all p with $1 < p < 3/2$, there exists a unique solution $u \in L^p(\Omega)$ to (2.3), which is the same for all p in this range.*

Remark 2.2. The same arguments used for the previous theorem allow us to prove the well-posedness of the problem in the 2D case; in such a case, we have existence and uniqueness of a solution $u \in L^p(\Omega)$ for each p with $1 < p < 2$.

2.2. Discrete problem. We assume that Ω is either a Lipschitz polyhedron (3D) or a Lipschitz polygon (2D).

We consider a regular family of tetrahedral (or triangular) meshes \mathcal{T}_h of Ω (see, for instance, [5]). As usual, h denotes the mesh size: $h := \max_{T \in \mathcal{T}_h} h_T$, h_T being the diameter of T . We consider the space of Lagrange finite elements of degree one:

$$H_h := \{v_h \in \mathcal{C}(\Omega) : v_h|_T \in \mathcal{P}_1 \ \forall T \in \mathcal{T}_h\}.$$

(\mathcal{P}_k denotes the set of polynomials with degree not larger than $k \in \mathbb{N}$.) Notice that $H_h \subset L^p(\Omega)$ for all $p \geq 1$.

Let $T_0 \in \mathcal{T}_h$ be such that $\mathbf{x}_0 \in T_0$. Usually \mathbf{x}_0 will be an inner point of an element of \mathcal{T}_h , however if \mathbf{x}_0 belongs to more than one $T \in \mathcal{T}_h$, any element T_0 containing \mathbf{x}_0 can be chosen.

The finite element approximation of (2.3) reads: find $u_h \in H_h$ such that

$$(2.4) \quad \begin{cases} \int_{\Omega} \boldsymbol{\sigma} \nabla u_h \cdot \nabla v_h = \mathbf{p} \cdot \nabla (v_h|_{T_0})(\mathbf{x}_0) & \forall v_h \in H_h, \\ \int_{\Omega} u_h = 0. \end{cases}$$

Although some average of the gradients of different elements containing \mathbf{x}_0 could also be used, our analysis shows that the simplest minded approach of choosing a particular arbitrary element works fine.

To find an a priori error estimate in $L^p(\Omega)$, with $1 < p < 2$ in the 2D case and $1 < p < 3/2$ in the 3D case, we will use a duality argument. With this end, we consider the following auxiliary problem: given $\psi \in L^q(\Omega)$, find $\varphi \in H^1(\Omega)$ such that

$$(2.5) \quad \begin{cases} \operatorname{div}(\boldsymbol{\sigma} \nabla \varphi) = \psi - \frac{1}{|\Omega|} \int_{\Omega} \psi & \text{in } \Omega, \\ (\boldsymbol{\sigma} \nabla \varphi) \cdot \mathbf{n} = 0 & \text{on } \partial\Omega, \\ \int_{\Omega} \varphi = 0. \end{cases}$$

This problem is well-posed if $q > 1$ (2D case) or $q > 6/5$ (3D case). Since q will be the dual exponent of p , we will consider this problem for $q > 2$ (2D case) or $q > 3$ (3D case).

We will need the solution of this problem to be in $W^{2,q}(\Omega)$. This is true under suitable assumptions. First of all, we require that $\boldsymbol{\sigma} \in [C^1(\overline{\Omega})]^{2 \times 2}$ (note that this not a realistic assumption when modeling the brain conductivity, which presents

discontinuities across the different tissues). Moreover, we assume that Ω is *convex*. Then the arguments used to prove [8, Corollary 3.12] allow us to show that $\varphi \in W^{2,q}(\Omega)$ for each q such that $2 < q < q_0$, for a suitable q_0 (for the Laplace operator in the 2D case, it is known that $q_0 = \frac{2}{2-\pi/\theta}$, θ being the largest inner angle of Ω). Moreover

$$(2.6) \quad \|\varphi\|_{2,q,\Omega} \leq C\|\psi\|_{0,q,\Omega}.$$

We do not know if, for a general convex polyhedron, one has $q_0 > 3$. Therefore, despite the original problem is set in the 3D case, from now on we will present our results in the 2D framework. In Section 5, we will extend them to the 3D case, although under additional stringent assumptions. So, in the following we will consider a convex Lipschitz polygon $\Omega \subset \mathbb{R}^2$.

In what follows we will denote $v^I \in H_h$ the Lagrange interpolant of v . Notice that, in particular, φ^I is well defined because $\varphi \in W^{2,q}(\Omega)$. Let us recall the following 2D interpolation error estimates. For their proof see, e.g., [3, Theorem 4.4.4 and Corollary 4.4.7].

Proposition 2.3. *Suppose $1 < q \leq \infty$ and $m > \frac{2}{q}$. Then, for $0 \leq i \leq m$ and $v \in W^{m,q}(T)$, $T \in \mathcal{T}_h$, we have*

$$(2.7) \quad |v - v^I|_{i,q,T} \leq Ch_T^{m-i} |v|_{m,q,T},$$

$$(2.8) \quad |v - v^I|_{i,\infty,T} \leq Ch_T^{m-i-2/q} |v|_{m,q,T}.$$

Here and thereafter C , as well as C' , denote strictly positive constants, not necessarily the same at each occurrence, but always independent of the mesh size.

Moreover we have the following error estimate for the elliptic projection:

Lemma 2.4. *Let Ω be a convex Lipschitz polygon. Let $\{\mathcal{T}_h\}$ be a quasiuniform family of subdivisions of Ω (namely, there exists a positive constant τ , independent of h , such that $\tau h \leq h_T \leq h$ for all $T \in \mathcal{T}_h$ and for all \mathcal{T}_h). Assume that $\sigma \in [C^1(\bar{\Omega})]^{2 \times 2}$. Consider a function $\xi \in W^{2,q}(\Omega)$ for $q > 2$ and let $\xi^P \in H_h$ be the unique solution of*

$$(2.9) \quad \begin{cases} \int_{\Omega} \sigma \nabla v_h \cdot \nabla \xi^P = \int_{\Omega} \sigma \nabla v_h \cdot \nabla \xi & \forall v_h \in H_h, \\ \int_{\Omega} \xi^P = 0. \end{cases}$$

Then there exists $h_0 > 0$ such that

$$(2.10) \quad |\xi - \xi^P|_{1,\infty,T} \leq Ch^{1-2/q} \|\xi\|_{2,q,\Omega} \quad \forall T \in \mathcal{T}_h$$

for $0 < h < h_0$.

Proof. This is a standard estimate for the elliptic projection; we include a brief proof for completeness. We consider an arbitrary $T \in \mathcal{T}_h$. Using (2.8) and an inverse estimate (see [3, Lemma 4.5.3]) we have

$$\begin{aligned} |\xi - \xi^P|_{1,\infty,T} &\leq |\xi - \xi^I|_{1,\infty,T} + |(\xi - \xi^P)^I|_{1,\infty,T} \\ &\leq C \left(h_T^{1-2/q} |\xi|_{2,q,T} + h_T^{-2/q} \|(\xi - \xi^P)^I\|_{1,q,T} \right). \end{aligned}$$

On the other hand,

$$\|(\xi - \xi^P)^I\|_{1,q,\Omega} \leq \|\xi - \xi^I\|_{1,q,\Omega} + \|\xi - \xi^P\|_{1,q,\Omega} \leq Ch|\xi|_{2,q,\Omega}$$

(see, for instance, [3, Theorem 4.4.4 and equation (8.5.4)]), and the desired result follows by using the quasiuniformity of the meshes. \square

Now we are in a position to prove an a priori error estimate for the proposed finite element scheme.

Theorem 2.5. *Let \mathcal{T}_h be a quasiuniform family of subdivisions of the convex Lipschitz polygon Ω and assume that $\sigma_{i,j} \in C^1(\bar{\Omega})$ for each $i, j = 1, 2$. Let u and u_h be the respective solutions to problems (2.3) and (2.4). Then there exists $h_0 > 0$ such that*

$$\|u - u_h\|_{0,p,\Omega} \leq Ch^{2/p-1}$$

for all $0 < h < h_0$ and for all p such that $\frac{q_0}{q_0-1} < p < 2$, where q_0 is the maximal regularity exponent in (2.6). Moreover, for $1 \leq p \leq \frac{q_0}{q_0-1}$ it holds

$$\|u - u_h\|_{0,p,\Omega} \leq Ch^s$$

for all $0 < h < h_0$ and for all s with $0 < s < 1 - \frac{2}{q_0}$.

Proof. Given $\psi \in L^q(\Omega)$ with $\frac{1}{p} + \frac{1}{q} = 1$, we know that the solution φ of (2.5) satisfies $\varphi \in W^{2,q}(\Omega)$ for $2 < q < q_0$. By using (2.3) and integration by parts, we obtain

$$\begin{aligned} (2.11) \quad \int_{\Omega} (u - u_h)\psi &= \int_{\Omega} (u - u_h) \left(\operatorname{div}(\boldsymbol{\sigma}\nabla\varphi) + \frac{1}{|\Omega|} \int_{\Omega} \psi \right) \\ &= \int_{\Omega} u \operatorname{div}(\boldsymbol{\sigma}\nabla\varphi) - \int_{\Omega} u_h \operatorname{div}(\boldsymbol{\sigma}\nabla\varphi) \\ &= -\boldsymbol{p} \cdot \nabla\varphi(\boldsymbol{x}_0) + \int_{\Omega} \boldsymbol{\sigma}\nabla u_h \cdot \nabla\varphi \\ &= -\boldsymbol{p} \cdot \nabla\varphi(\boldsymbol{x}_0) + \int_{\Omega} \boldsymbol{\sigma}\nabla u_h \cdot \nabla\varphi^P \\ &= -\boldsymbol{p} \cdot \nabla\varphi(\boldsymbol{x}_0) + \boldsymbol{p} \cdot \nabla(\varphi^P|_{T_0})(\boldsymbol{x}_0), \end{aligned}$$

where φ^P is the unique solution to problem (2.9) (with φ at the right hand side instead of ξ). From Lemma 2.4 we have

$$|\nabla\varphi(\boldsymbol{x}_0) - \nabla\varphi^P(\boldsymbol{x}_0)| \leq Ch^{1-2/q}\|\varphi\|_{2,q,\Omega} \leq Ch^{1-2/q}\|\psi\|_{0,q,\Omega},$$

where the last inequality follows from (2.6). Therefore we have

$$\|u - u_h\|_{0,p,\Omega} = \sup_{\psi \in L^q(\Omega)} \frac{\int_{\Omega} (u - u_h)\psi}{\|\psi\|_{0,q,\Omega}} \leq Ch^{1-2/q} = Ch^{2/p-1}.$$

The last assertion follows from the Hölder inequality and the previous estimate, as

$$\|u - u_h\|_{0,p,\Omega} \leq C\|u - u_h\|_{0,r,\Omega} \leq Ch^{2/r-1}$$

for each r with $\frac{q_0}{q_0-1} < r < 2$. \square

The quasiuniformity assumption on the meshes seems unfitting for this problem, because the strong singularity of the solution at \boldsymbol{x}_0 suggests using meshes highly refined in the vicinity of this point. In what follows we will introduce a posteriori estimators of the L^p norm of the error which will be proved to be efficient and reliable without the need of the quasiuniformity assumption. Later on these estimates

will be used to devise an adaptive scheme which will lead to an optimal order of convergence in terms of the number of degrees of freedom.

3. PRELIMINARY RESULTS

For the a posteriori analysis, we will have to deal with three kinds of bubble functions, one associated with triangles, another associated with edges and the last one associated with the point \mathbf{x}_0 . In this section we introduce these bubble functions and prove some properties that will be used in the sequel. From now on \mathbf{n} will denote a generic unit vector normal to a curve which will be clear from the context.

Let b_T be the bubble function with support in T defined in Ω by

$$(3.1) \quad b_T(\mathbf{x}) := \begin{cases} (\lambda_1^T \lambda_2^T \lambda_3^T)^2 \frac{|\mathbf{x} - \mathbf{x}_0|^2}{h_T^2} & \text{if } \mathbf{x}_0 \in T \\ (\lambda_1^T \lambda_2^T \lambda_3^T)^2 & \text{otherwise.} \end{cases}$$

where λ_i^T is the barycentric coordinate of \mathbf{x} associated with the triangle T and its vertex P_i , $i = 1, 2, 3$. The function b_T have the following properties:

Lemma 3.1. *Given $T \in \mathcal{T}_h$, let b_T be defined as above. Then*

$$(3.2) \quad 0 \leq b_T \leq 1,$$

$$(3.3) \quad b_T = 0 \quad \text{on} \quad \partial T,$$

$$(3.4) \quad \nabla b_T = 0 \quad \text{on} \quad \partial T,$$

$$(3.5) \quad \int_T b_T \geq C|T|,$$

$$(3.6) \quad \|b_T\|_{2,q,T} \leq C|T|^{-1/p}.$$

Proof. Equations (3.2), (3.3), and (3.4) are immediate consequences of the definition of b_T . Estimate (3.5) follows from straightforward computations and (3.6) from standard scaling arguments (see [6, Theorem 15.1]):

$$\|b_T\|_{2,q,T} \leq Ch_T^{-4/p} \|b_T\|_{0,p,T} \leq Ch_T^{-2/p} \leq C|T|^{-1/p}.$$

□

Let $\mathcal{E}_{h,i}$ be the set of all the inner edges and $\mathcal{E}_{h,e}$ the set of boundary edges of the triangulation \mathcal{T}_h . Given $\ell \in \mathcal{E}_h := \mathcal{E}_{h,i} \cup \mathcal{E}_{h,e}$ we will define a bubble function with support $\omega_\ell := \{T \in \mathcal{T}_h : \ell \subset \partial T\}$ (see Figure 1).

In the case $\ell \in \mathcal{E}_{h,i}$ we define b_ℓ for $\mathbf{x} \in \omega_\ell$ by

$$(3.7) \quad b_\ell(\mathbf{x}) := \begin{cases} \left(\lambda_2^{T_1} \lambda_3^{T_1} \lambda_2^{T_2} \lambda_3^{T_2} \right)^2 \frac{|\mathbf{x} - \mathbf{x}_0|^2}{|\ell|^2} & \text{if } \mathbf{x}_0 \in \omega_\ell \\ \left(\lambda_2^{T_1} \lambda_3^{T_1} \lambda_2^{T_2} \lambda_3^{T_2} \right)^2 & \text{if } \mathbf{x}_0 \notin \omega_\ell, \end{cases}$$

where $|\ell|$ denotes the length of ℓ . Since $\lambda_i^{T_j}$ is a linear function in the whole plane, b_ℓ is a polynomial in ω_ℓ .

It remains to define bubble functions b_ℓ for $\ell \in \mathcal{E}_{h,e}$, which, in particular, must satisfy

$$(\boldsymbol{\sigma} \nabla b_\ell) \cdot \mathbf{n} = \nabla b_\ell \cdot (\boldsymbol{\sigma} \mathbf{n}) = 0 \quad \text{on } \ell \quad \text{for all } \ell \in \mathcal{E}_{h,e}.$$

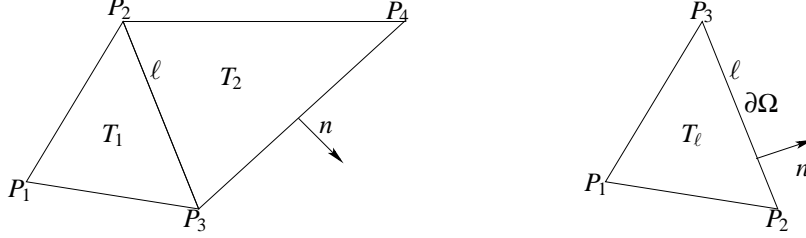


FIGURE 1. The support ω_ℓ of b_ℓ with $\ell \in \mathcal{E}_{h,i}$ and $\ell \in \mathcal{E}_{h,e}$.

Let T_ℓ be the triangle in \mathcal{T}_h that contains ℓ . For simplicity we assume that $\mathbf{x}_0 \notin T_\ell$. Let (x_i, y_i) be the coordinates of the vertices P_i , $i = 1, 2, 3$, of the triangle T_ℓ , as shown in Figure 2. Let $F_\ell : \mathbb{R}^2 \rightarrow \mathbb{R}^2$ be defined by

$$F_\ell \begin{pmatrix} \hat{x} \\ \hat{y} \end{pmatrix} = \begin{pmatrix} x_2 \\ y_2 \end{pmatrix} + Q \begin{pmatrix} \hat{x} \\ \hat{y} \end{pmatrix}$$

where $Q = \begin{pmatrix} x_3 - x_2 & -(y_3 - y_2) \\ y_3 - y_2 & x_3 - x_2 \end{pmatrix}$. Notice that $Q = |\ell| (\mathbf{t} \quad -\mathbf{n})$ (see Figure 2) and that $Q^t Q = |\ell|^2 I$. Hence, denoting $\hat{T}_\ell := F_\ell^{-1}(T_\ell)$, the triangles \hat{T}_ℓ and T_ℓ are similar (in particular, both have the same aspect ratio). Let us set $\hat{\sigma} := Q^t(\sigma \circ F_\ell)Q$; this matrix is symmetric and positive definite for all $(\hat{x}, \hat{y}) \in \hat{T}_\ell$. It is easy to show that there exists $\delta > 0$ such that $[1/2 - \delta, 1/2 + \delta] \times (0, 2\delta]$ is contained in the interior of \hat{T}_ℓ (see Figure 3). Since δ only depends on the aspect ratio of the triangle \hat{T}_ℓ , hence of that of T_ℓ , it can be bounded from above and from below by two positive constants, uniformly with respect to h . Now let $g_1 \in \mathcal{D}((1/2 - \delta, 1/2 + \delta))$ be such that $g_1 \geq 0$ and $\int_{\mathbb{R}} g_1 = 1$, and let $g_2 \in \mathcal{C}^\infty(\mathbb{R})$ be such that $0 \leq g_2 \leq 1$, $g_2|_{(-\infty, \delta)} = 1$, $g_2|_{(2\delta, +\infty)} = 0$ and $|g_2'| \leq C\delta^{-1}$. We first define

$$\hat{b}(\hat{x}, \hat{y}) := g_1(\hat{x}) - g_1(\hat{x}) \frac{\hat{\sigma}_{12}(\hat{x}, 0)}{\hat{\sigma}_{22}(\hat{x}, 0)} g_2(\hat{y}) \hat{y},$$

then

$$(3.8) \quad b_\ell := \hat{b} \circ F_\ell^{-1}|_{T_\ell}.$$

Notice that $\hat{\sigma}_{22}(\hat{x}, 0)$ cannot vanish because $\hat{\sigma}$ is positive definite. Since $\frac{\partial \hat{b}}{\partial \hat{x}}(\hat{x}, 0) = g_1'(\hat{x})$ and $\frac{\partial \hat{b}}{\partial \hat{y}}(\hat{x}, 0) = -g_1(\hat{x}) \frac{\hat{\sigma}_{12}(\hat{x}, 0)}{\hat{\sigma}_{22}(\hat{x}, 0)}$, straightforward computations allow us to show that $(\sigma \mathbf{n})^t \nabla b_\ell = |\ell|^{-2} (\hat{\sigma} \hat{\mathbf{n}})^t \hat{\nabla} \hat{b} = 0$.

Now it is easy to prove the following result for b_ℓ :

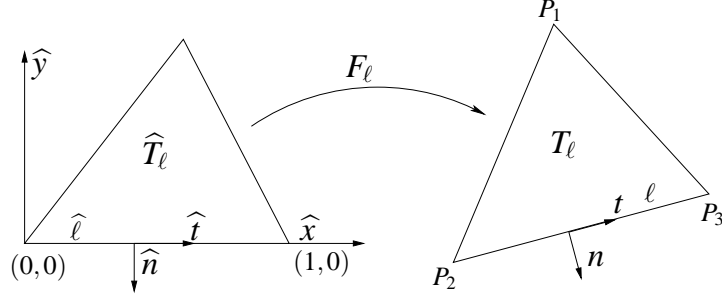
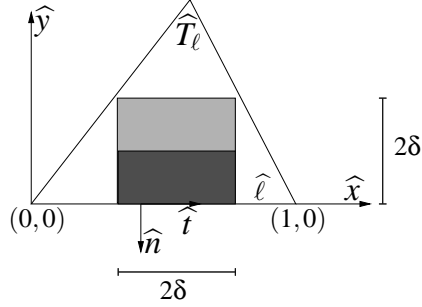
Lemma 3.2. *Given $\ell \in \mathcal{E}_h$, let b_ℓ and ω_ℓ be defined as above. Then*

$$(3.9) \quad b_\ell|_{\ell^*} = 0 \quad \forall \ell^* \in \mathcal{E}_h, \ell^* \neq \ell,$$

$$(3.10) \quad (\sigma \nabla b_\ell) \cdot \mathbf{n} = 0 \quad \text{on } \partial \omega_\ell,$$

$$(3.11) \quad C|\ell| \leq \int_\ell b_\ell \leq C'|\ell|,$$

$$(3.12) \quad |b_\ell|_{m,q,\omega_\ell} \leq C|\ell|^{2-m-2/p}, \quad m = 0, 1, 2.$$


FIGURE 2. The definition of F_ℓ .

FIGURE 3. The support of b_ℓ .

Proof. For the case $\ell \in \mathcal{E}_{h,i}$, the proof runs essentially identical to that of [1, Lemma 3.1]. For $\ell \in \mathcal{E}_{h,e}$ the first three properties have already been checked. The last one follows from standard scaling arguments. \square

The third kind of bubble function concerns the point \mathbf{x}_0 and the triangle T_0 that we have chosen such that $\mathbf{x}_0 \in T_0$. We will denote by h_0 the diameter of T_0 . Let us set

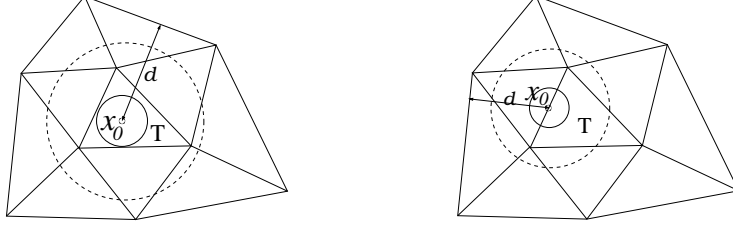
$$(3.13) \quad \omega_{T_0} := \{T' \in \mathcal{T}_h : T' \cap T_0 \neq \emptyset\}$$

and $d := \text{dist}(\mathbf{x}_0, \partial\omega_{T_0})$ (since \mathbf{x}_0 is an inner point of Ω then $d > 0$). Notice that, because of the regularity of the mesh, there exist two positive constants such that $Ch_0 \leq d \leq C'h_0$. Let $\chi(\mathbf{x})$ be the convolution of the characteristic function of the set $\{\mathbf{x} \in \Omega : |\mathbf{x} - \mathbf{x}_0| < d/2\}$ with an appropriate mollifier, so that $\chi(\mathbf{x}) = 1$ if $|\mathbf{x} - \mathbf{x}_0| \leq d/4$, $\chi(\mathbf{x}) = 0$ if $|\mathbf{x} - \mathbf{x}_0| \geq 3d/4$ and $|\nabla\chi(\mathbf{x})| \leq Cd^{-1}$.

We define the bubble function

$$(3.14) \quad b_0(\mathbf{x}) := \mathbf{p} \cdot (\mathbf{x} - \mathbf{x}_0) \chi(\mathbf{x}).$$

The support of b_0 is contained in ω_{T_0} . Moreover the following results hold true:

FIGURE 4. Two examples of ω_{T_0} .

Lemma 3.3. *Let b_0 be defined as above. Then*

$$(3.15) \quad \nabla b_0(\mathbf{x}_0) = \mathbf{p},$$

$$(3.16) \quad \nabla b_0 = 0 \quad \text{on } \partial\omega_{T_0},$$

$$(3.17) \quad b_0(\mathbf{x}) = \mathbf{p} \cdot (\mathbf{x} - \mathbf{x}_0) \quad \forall \mathbf{x} \in \Omega : |\mathbf{x} - \mathbf{x}_0| \leq \frac{d}{4},$$

$$(3.18) \quad b_0(\mathbf{x}) = 0 \quad \forall \mathbf{x} \in \Omega : |\mathbf{x} - \mathbf{x}_0| \geq \frac{3d}{4},$$

$$(3.19) \quad |b_0|_{m,\infty,\omega_{T_0}} \leq Cd^{1-m}, \quad m = 0, 1, 2.$$

Proof. It follows from straightforward calculations. In particular, (3.19) follows by combining that $|\chi|_{m,\infty,\omega_{T_0}} \leq Cd^{-m}$ (see [1, equation (3.8)]) with the fact that $\mathbf{p} \cdot (\mathbf{x} - \mathbf{x}_0)$ is linear and continuous. \square

Corollary 3.4. *Let b_0 and ω_{T_0} be defined as above. Then,*

$$|b_0|_{m,q,\omega_{T_0}} \leq Ch_0^{3-m-2/p}, \quad m = 0, 1, 2,$$

and, for all edge ℓ ,

$$\|b_0\|_{0,q,\ell} \leq C|\ell|^{2-1/p}.$$

Proof. Using (3.19) and the fact that $h_0 \leq Cd \leq Ch_0$, we have

$$|b_0|_{m,q,\omega_{T_0}} \leq |b_0|_{m,\infty,\omega_{T_0}} |\omega_{T_0}|^{1/q} \leq Cd^{1-m} h_0^{2/q} \leq Ch_0^{3-m-2/p}.$$

Moreover, using that

$$\|v\|_{0,q,\partial T} \leq C\|v\|_{0,q,T}^{1-1/q} \|v\|_{1,q,T}^{1/q} \quad \forall v \in W^{1,q}(T)$$

(see [3, Theorem 1.6.6]), we have

$$\|b_0\|_{0,q,\ell} \leq C\|b_0\|_{0,q,\omega_{T_0}}^{1-1/q} \|b_0\|_{1,q,\omega_{T_0}}^{1/q} \leq C|\ell|^{(3-2/p)(1-1/q)} |\ell|^{(2-2/p)(1/q)} = C|\ell|^{2-1/p}.$$

\square

To end this section, we recall an error estimate for the Lagrange interpolant $v^I \in H_h$ of a function $v \in \mathcal{C}(\bar{\Omega})$.

Lemma 3.5. *Given $\ell \in \mathcal{E}_h$, let ω_ℓ be defined as above. There holds*

$$\|v - v^I\|_{0,q,\ell} \leq C|\ell|^{1+1/p} |v|_{2,q,\omega_\ell} \quad \forall v \in W^{2,q}(\omega_\ell), \quad 1 < q < \infty.$$

Proof. See, for instance, [1, Lemma 3.4]. \square

4. AN A POSTERIORI ERROR ESTIMATOR

According to Remark 2.2 the solution of problem (2.3) belongs to $L^p(\Omega)$ with $1 \leq p < 2$. In this section we will define an a posteriori error estimator in the $L^p(\Omega)$ -norm for the finite element approximation error $u - u_h$. We will prove the reliability and efficiency of the estimator for a particular range of p . Let us emphasize that this proof holds for a regular family of meshes and does not need the quasiuniformity assumption, so that the error estimator can be used to drive an adaptive scheme.

For all $T \in \mathcal{T}_h$ we define

$$\varepsilon_{T,p} := \left(h_T^{2p} \|\operatorname{div}(\boldsymbol{\sigma} \nabla u_h)\|_{0,p,T}^p + \frac{1}{2} \sum_{\ell \in \mathcal{E}(T) \cap \mathcal{E}_{h,i}} |\ell|^{p+1} \|[[\boldsymbol{\sigma} \nabla u_h \cdot \mathbf{n}]]\|_{0,p,\ell}^p + \sum_{\ell \in \mathcal{E}(T) \cap \mathcal{E}_{h,e}} |\ell|^{p+1} \|\boldsymbol{\sigma} \nabla u_h \cdot \mathbf{n}\|_{0,p,\ell}^p \right)^{1/p},$$

where $\mathcal{E}(T)$ is the set of the edges of T and $[[g]]$ denotes the jump of g across an edge. We define the local a posteriori error indicator $\eta_{T,p}$ for all $T \in \mathcal{T}_h$ as follows:

$$\eta_{T,p} := \begin{cases} \left(h_0^{2-p} + \varepsilon_{T_0,p}^p \right)^{1/p} & \text{if } T = T_0, \\ \varepsilon_{T,p} & \text{otherwise.} \end{cases}$$

Next, we define the global error estimator from these indicators as follows:

$$\eta_p := \left(\sum_{T \in \mathcal{T}_h} \eta_{T,p}^p \right)^{1/p}.$$

4.1. Reliability. To show that this estimator is reliable, we prove the following theorem which is based on a duality argument as that used for Theorem 2.5.

Theorem 4.1. *Let Ω be a convex Lipschitz polygon and let $\sigma_{i,j} \in C^1(\overline{\Omega})$ for each $i, j = 1, 2$. Let η_p be defined as above with $p \in (\frac{q_0}{q_0-1}, 2)$, where $q_0 > 2$ is the maximal regularity exponent in (2.6). Then, the following estimate holds true:*

$$\|u - u_h\|_{0,p,\Omega} \leq C \eta_p.$$

Proof. Given $\psi \in L^q(\Omega)$, let $\varphi \in W^{2,q}(\Omega)$ be the solution of (2.5). Proceeding as in (2.11), using (2.4) tested with $v_h = \varphi^I$ (the Lagrange interpolant of φ), and integrating by parts, we obtain

$$\begin{aligned} (4.1) \quad \int_{\Omega} (u - u_h) \psi &= -\mathbf{p} \cdot \nabla \varphi(\mathbf{x}_0) + \int_{\Omega} \boldsymbol{\sigma} \nabla u_h \cdot \nabla \varphi \\ &= \mathbf{p} \cdot (\nabla \varphi^I(\mathbf{x}_0) - \nabla \varphi(\mathbf{x}_0)) + \int_{\Omega} \boldsymbol{\sigma} \nabla u_h \cdot \nabla (\varphi - \varphi^I) \\ &= \mathbf{p} \cdot (\nabla \varphi^I(\mathbf{x}_0) - \nabla \varphi(\mathbf{x}_0)) - \sum_{T \in \mathcal{T}_h} \int_T \operatorname{div}(\boldsymbol{\sigma} \nabla u_h) (\varphi - \varphi^I) \\ &\quad + \sum_{\ell \in \mathcal{E}_{h,i}} \int_{\ell} [[\boldsymbol{\sigma} \nabla u_h \cdot \mathbf{n}]] (\varphi - \varphi^I) + \sum_{\ell \in \mathcal{E}_{h,e}} \int_{\ell} \boldsymbol{\sigma} \nabla u_h \cdot \mathbf{n} (\varphi - \varphi^I). \end{aligned}$$

Using Hölder inequality, Proposition 2.3, and Lemma 3.5 we estimate each term on the right hand side as follows:

$$|\mathbf{p} \cdot \nabla(\varphi - \varphi^I)(\mathbf{x}_0)| \leq |\mathbf{p}| |\varphi - \varphi^I|_{1,\infty,T_0} \leq Ch_0^{1-2/q} |\varphi|_{2,q,T_0},$$

$$\begin{aligned} \sum_{T \in \mathcal{T}_h} \int_T \operatorname{div}(\boldsymbol{\sigma} \nabla u_h)(\varphi - \varphi^I) &\leq \sum_{T \in \mathcal{T}_h} \|\operatorname{div}(\boldsymbol{\sigma} \nabla u_h)\|_{0,p,T} \|\varphi - \varphi^I\|_{0,q,T} \\ &\leq C \sum_{T \in \mathcal{T}_h} h_T^2 \|\operatorname{div}(\boldsymbol{\sigma} \nabla u_h)\|_{0,p,T} |\varphi|_{2,q,T} \\ &\leq C \left(\sum_{T \in \mathcal{T}_h} h_T^{2p} \|\operatorname{div}(\boldsymbol{\sigma} \nabla u_h)\|_{0,p,T}^p \right)^{1/p} |\varphi|_{2,q,\Omega}, \end{aligned}$$

$$\begin{aligned} \sum_{\ell \in \mathcal{E}_{h,i}} \int_{\ell} [\boldsymbol{\sigma} \nabla u_h \cdot \mathbf{n}](\varphi - \varphi^I) &\leq \sum_{\ell \in \mathcal{E}_{h,i}} \|[\boldsymbol{\sigma} \nabla u_h \cdot \mathbf{n}]\|_{0,p,\ell} \|\varphi - \varphi^I\|_{0,q,\ell} \\ &\leq C \sum_{\ell \in \mathcal{E}_{h,i}} |\ell|^{1+1/p} \|[\boldsymbol{\sigma} \nabla u_h \cdot \mathbf{n}]\|_{0,p,\ell} |\varphi|_{2,q,\omega_\ell} \\ &\leq C \left(\sum_{\ell \in \mathcal{E}_{h,i}} |\ell|^{p+1} \|[\boldsymbol{\sigma} \nabla u_h \cdot \mathbf{n}]\|_{0,p,\ell}^p \right)^{1/p} |\varphi|_{2,q,\Omega}, \end{aligned}$$

$$\begin{aligned} \sum_{\ell \in \mathcal{E}_{h,e}} \int_{\ell} \boldsymbol{\sigma} \nabla u_h \cdot \mathbf{n}(\varphi - \varphi^I) &\leq \sum_{\ell \in \mathcal{E}_{h,e}} \|\boldsymbol{\sigma} \nabla u_h \cdot \mathbf{n}\|_{0,p,\ell} \|\varphi - \varphi^I\|_{0,q,\ell} \\ &\leq C \sum_{\ell \in \mathcal{E}_{h,e}} |\ell|^{1+1/p} \|\boldsymbol{\sigma} \nabla u_h \cdot \mathbf{n}\|_{0,p,\ell} |\varphi|_{2,q,\omega_\ell} \\ &\leq C \left(\sum_{\ell \in \mathcal{E}_{h,e}} |\ell|^{p+1} \|\boldsymbol{\sigma} \nabla u_h \cdot \mathbf{n}\|_{0,p,\ell}^p \right)^{1/p} |\varphi|_{2,q,\Omega}. \end{aligned}$$

Substituting all these estimates in (4.1) and using (2.6), we obtain

$$\begin{aligned} \int_{\Omega} (u - u_h) \psi &\leq C \left(h_0^{2-p} + \sum_{T \in \mathcal{T}_h} h_T^{2p} \|\operatorname{div}(\boldsymbol{\sigma} \nabla u_h)\|_{0,p,T}^p \right. \\ &\quad \left. + \sum_{\ell \in \mathcal{E}_{h,i}} |\ell|^{p+1} \|[\boldsymbol{\sigma} \nabla u_h \cdot \mathbf{n}]\|_{0,p,\ell}^p + \sum_{\ell \in \mathcal{E}_{h,e}} |\ell|^{p+1} \|\boldsymbol{\sigma} \nabla u_h \cdot \mathbf{n}\|_{0,p,\ell}^p \right)^{1/p} \|\psi\|_{0,q,\Omega}. \end{aligned}$$

Therefore,

$$\begin{aligned} \|u - u_h\|_{0,p,\Omega} &= \sup_{\psi \in L^q(\Omega)} \frac{\int_{\Omega} (u - u_h)\psi}{\|\psi\|_{0,q,\Omega}} \\ &\leq C \left(h_0^{2-p} + \sum_{T \in \mathcal{T}_h} h_T^{2p} \|\operatorname{div}(\boldsymbol{\sigma} \nabla u_h)\|_{0,p,T}^p + \sum_{\ell \in \mathcal{E}_{h,i}} |\ell|^{p+1} \|[\boldsymbol{\sigma} \nabla u_h \cdot \mathbf{n}]\|_{0,p,\ell}^p \right. \\ &\quad \left. + \sum_{\ell \in \mathcal{E}_{h,e}} |\ell|^{p+1} \|\boldsymbol{\sigma} \nabla u_h \cdot \mathbf{n}\|_{0,p,\ell}^p \right)^{1/p} \end{aligned}$$

and from this we conclude the theorem. \square

4.2. Efficiency. In this subsection we always assume that $\sigma_{i,j} \in C^1(\bar{\Omega})$ for each $i, j = 1, 2$.

To prove the efficiency estimate, we will use some techniques that appears in [12]. For that, we introduce the matrix $\boldsymbol{\sigma}^I$, whose entries are the Lagrange interpolants of $\sigma_{i,j}$:

$$\boldsymbol{\sigma}^I := (\sigma_{i,j}^I)_{1 \leq i,j \leq 2}.$$

The following four lemmas provide upper bounds for each term defining $\eta_{T,p}^p$. Here and thereafter $\operatorname{div}(\cdot)$ must be understood in the following row-wise sense: $(\operatorname{div}(\boldsymbol{\sigma}))_j = \sum_i \frac{\partial \sigma_{i,j}}{\partial x_i}$.

Lemma 4.2. *The following estimate holds true:*

$$h_T^{2p} \|\operatorname{div}(\boldsymbol{\sigma} \nabla u_h)\|_{0,p,T}^p \leq C \left(\|\boldsymbol{\sigma}\|_{1,\infty,T}^p \|u - u_h\|_{0,p,T}^p + h_T^{2p} \|[\operatorname{div}(\boldsymbol{\sigma} - \boldsymbol{\sigma}^I)] \cdot \nabla u_h\|_{0,p,T}^p \right)$$

for all $T \in \mathcal{T}_h$.

Proof. Let us consider an arbitrary $T \in \mathcal{T}_h$, the bubble function b_T defined in (3.1) and the function ψ_T defined in Ω as

$$\psi_T := \operatorname{div}(\boldsymbol{\sigma}^I \nabla u_h) b_T \quad \text{in } T.$$

Like b_T , this function is supported in T .

The fact that $\operatorname{div}(\boldsymbol{\sigma}^I \nabla u_h)|_T \in \mathcal{P}_0$, (3.5), (3.3), (3.4), and integration by parts yield

$$\begin{aligned} \|\operatorname{div}(\boldsymbol{\sigma}^I \nabla u_h)\|_{0,p,T}^2 &= |T|^{2/p-1} \|\operatorname{div}(\boldsymbol{\sigma}^I \nabla u_h)\|_{0,2,T}^2 \\ &\leq C |T|^{2/p-1} \|b_T^{1/2} \operatorname{div}(\boldsymbol{\sigma}^I \nabla u_h)\|_{0,2,T}^2 \\ &= C |T|^{2/p-1} \left(\int_T \operatorname{div}(\boldsymbol{\sigma} \nabla u_h) \psi_T + \int_T \operatorname{div}((\boldsymbol{\sigma}^I - \boldsymbol{\sigma}) \nabla u_h) \psi_T \right) \\ &= C |T|^{2/p-1} \left(\int_T u_h \operatorname{div}(\boldsymbol{\sigma} \nabla \psi_T) + \int_T [\operatorname{div}(\boldsymbol{\sigma}^I - \boldsymbol{\sigma})] \cdot \nabla u_h \psi_T \right). \end{aligned}$$

Next we notice that, since u is solution of (2.3) and $\nabla b_T(\mathbf{x}_0) = 0$, one has

$$\int_T u \operatorname{div}(\boldsymbol{\sigma} \nabla \psi_T) = -\mathbf{p} \cdot \nabla \psi_T(\mathbf{x}_0) = 0.$$

Therefore, we can write

$$\begin{aligned} \|\operatorname{div}(\boldsymbol{\sigma}^I \nabla u_h)\|_{0,p,T}^2 &\leq C |T|^{2/p-1} \left(\int_T (u_h - u) \operatorname{div}(\boldsymbol{\sigma} \nabla \psi_T) + \int_T [\operatorname{div}(\boldsymbol{\sigma}^I - \boldsymbol{\sigma})] \cdot \nabla u_h \psi_T \right). \end{aligned}$$

For the first term we have

$$\left| \int_T (u_h - u) \operatorname{div}(\boldsymbol{\sigma} \nabla \psi_T) \right| \leq 2 \|u - u_h\|_{0,p,T} \|\boldsymbol{\sigma}\|_{1,\infty,T} \|\psi_T\|_{2,q,T}$$

and, using (3.6),

$$\begin{aligned} \|\psi_T\|_{2,q,T} &= \|\operatorname{div}(\boldsymbol{\sigma}^I \nabla u_h)\| \|b_T\|_{2,q,T} \\ &\leq C |\operatorname{div}(\boldsymbol{\sigma}^I \nabla u_h)| |T|^{-1/p} \leq C \|\operatorname{div}(\boldsymbol{\sigma}^I \nabla u_h)\|_{0,p,T} |T|^{-2/p}. \end{aligned}$$

For the second one,

$$\left| \int_T [\mathbf{div}(\boldsymbol{\sigma}^I - \boldsymbol{\sigma})] \cdot \nabla u_h \psi_T \right| \leq \|[\mathbf{div}(\boldsymbol{\sigma}^I - \boldsymbol{\sigma})] \cdot \nabla u_h\|_{0,p,T} \|\psi_T\|_{0,q,T}$$

and, now using (3.2),

$$\|\psi_T\|_{0,q,T} \leq C |\operatorname{div}(\boldsymbol{\sigma}^I \nabla u_h)| |T|^{1/q} \leq C \|\operatorname{div}(\boldsymbol{\sigma}^I \nabla u_h)\|_{0,p,T} |T|^{1/q-1/p}.$$

Hence

$$\|\operatorname{div}(\boldsymbol{\sigma}^I \nabla u_h)\|_{0,p,T} \leq C (h_T^{-2} \|\boldsymbol{\sigma}\|_{1,\infty,T} \|u - u_h\|_{0,p,T} + \|[\mathbf{div}(\boldsymbol{\sigma}^I - \boldsymbol{\sigma})] \cdot \nabla u_h\|_{0,p,T})$$

from which we easily obtain the desired result. \square

Lemma 4.3. *The following estimate holds true*

$$\begin{aligned} &|\ell|^{p+1} \|[\boldsymbol{\sigma} \nabla u_h \cdot \mathbf{n}]\|_{0,p,\ell}^p \\ &\leq C \left(\|\boldsymbol{\sigma}\|_{1,\infty,\omega_\ell}^p \|u - u_h\|_{0,p,\omega_\ell}^p + \sum_{T' \subset \omega_\ell} h_{T'}^{2p} \|[\mathbf{div}(\boldsymbol{\sigma}^I - \boldsymbol{\sigma})] \cdot \nabla u_h\|_{0,p,T'}^p \right), \end{aligned}$$

for all $\ell \in \mathcal{E}_{h,i}$.

Proof. We consider an arbitrary $\ell \in \mathcal{E}_{h,i}$, the bubble function b_ℓ defined in (3.7) and

$$\psi_\ell := [\nabla u_h \cdot \mathbf{n}] b_\ell \quad \text{in } \Omega.$$

Like b_ℓ , this function is supported in ω_ℓ .

We know that the entries of $\boldsymbol{\sigma}$ belong to $L^\infty(\Omega)$ and, therefore, we have

$$(4.2) \quad \|[\boldsymbol{\sigma} \nabla u_h \cdot \mathbf{n}]\|_{0,p,\ell} \leq C \|[\nabla u_h \cdot \mathbf{n}]\|_{0,p,\ell} = C \|[\nabla u_h]\|_{0,p,\ell},$$

because the jump of the tangential component of ∇u_h is zero.

On the other hand, from (3.11) and the uniform positivity of $\boldsymbol{\sigma}$ we obtain

$$\begin{aligned} \|[\nabla u_h]_\ell\|_{0,p,\ell}^2 &= |\ell|^{2/p-1} \|[\nabla u_h]_\ell\|_{0,2,\ell}^2 \\ &\leq C |\ell|^{2/p-1} \|b_\ell^{1/2} [\nabla u_h]_\ell\|_{0,2,\ell}^2 \\ (4.3) \quad &\leq C |\ell|^{2/p-1} \int_\ell b_\ell [\nabla u_h]_\ell^t \boldsymbol{\sigma} [\nabla u_h]_\ell \\ &= C |\ell|^{2/p-1} \int_\ell [\boldsymbol{\sigma} \nabla u_h \cdot \mathbf{n}] \psi_\ell. \end{aligned}$$

Taking ψ_ℓ as a test function in (2.3), using that $\nabla b_\ell(\mathbf{x}_0) = \mathbf{0}$, integrating by parts, and recalling (3.9) and (3.10), we have

$$\begin{aligned} \int_{\omega_\ell} (u - u_h) \operatorname{div}(\boldsymbol{\sigma} \nabla \psi_\ell) &= - \sum_{T' \subset \omega_\ell} \int_{T'} u_h \operatorname{div}(\boldsymbol{\sigma} \nabla \psi_\ell) \\ &= - \sum_{T' \subset \omega_\ell} \int_{T'} \operatorname{div}(\boldsymbol{\sigma} \nabla u_h) \psi_\ell + \int_\ell [\boldsymbol{\sigma} \nabla u_h \cdot \mathbf{n}] \psi_\ell. \end{aligned}$$

Hence

$$\begin{aligned} \int_\ell [\boldsymbol{\sigma} \nabla u_h \cdot \mathbf{n}] \psi_\ell &= \sum_{T' \subset \omega_\ell} \int_{T'} \operatorname{div}(\boldsymbol{\sigma} \nabla u_h) \psi_\ell + \int_{\omega_\ell} (u - u_h) \operatorname{div}(\boldsymbol{\sigma} \nabla \psi_\ell) \\ (4.4) \quad &\leq C (\|\operatorname{div}(\boldsymbol{\sigma} \nabla \psi_\ell)\|_{0,q,\omega_\ell} \|u - u_h\|_{0,p,\omega_\ell} \\ &\quad + \sum_{T' \subset \omega_\ell} \|\operatorname{div}(\boldsymbol{\sigma} \nabla u_h)\|_{0,p,T'} \|\psi_\ell\|_{0,q,T'}) \\ &\leq C (\|\boldsymbol{\sigma}\|_{1,\infty,\omega_\ell} \|u - u_h\|_{0,p,\omega_\ell} \|\psi_\ell\|_{2,q,\omega_\ell} \\ &\quad + \sum_{T' \subset \omega_\ell} \|\operatorname{div}(\boldsymbol{\sigma} \nabla u_h)\|_{0,p,T'} \|\psi_\ell\|_{0,q,T'}) \end{aligned}$$

From standard scaling arguments and (3.12), we have

$$(4.5) \quad \|\psi_\ell\|_{0,q,\omega_\ell} \leq \|[\nabla u_h]_\ell\| \|b_\ell\|_{0,q,\omega_\ell} \leq C \|[\nabla u_h]_\ell\|_{0,p,\ell} |\ell|^{2-3/p}$$

and

$$(4.6) \quad \|\psi_\ell\|_{2,q,\omega_\ell} \leq C |\ell|^{-2} \|\psi_\ell\|_{0,q,\omega_\ell} \leq C \|[\nabla u_h]_\ell\|_{0,p,\ell} |\ell|^{-3/p}.$$

Hence, from (4.3) and (4.4), we write

$$\begin{aligned} \|[\nabla u_h]_\ell\|_{0,p,\ell} &\leq C |\ell|^{2/p-1} (|\ell|^{-3/p} \|\boldsymbol{\sigma}\|_{1,\infty,\omega_\ell} \|u - u_h\|_{0,p,\omega_\ell} \\ &\quad + \sum_{T' \subset \omega_\ell} |\ell|^{2-3/p} \|\operatorname{div}(\boldsymbol{\sigma} \nabla u_h)\|_{0,p,T'}) \end{aligned}$$

and, from (4.2),

$$\begin{aligned} |\ell|^{p+1} \|[\boldsymbol{\sigma} \nabla u_h \cdot \mathbf{n}]\|_{0,p,\ell}^p &\leq C (\|\boldsymbol{\sigma}\|_{1,\infty,\omega_\ell}^p \|u - u_h\|_{0,p,\omega_\ell}^p \\ &\quad + \sum_{T' \subset \omega_\ell} h_{T'}^{2p} \|\operatorname{div}(\boldsymbol{\sigma} \nabla u_h)\|_{0,p,T'}^p). \end{aligned}$$

We conclude the proof by using Lemma 4.2 to bound the last term. \square

Lemma 4.4. *The following estimate holds true*

$$\begin{aligned} |\ell|^{p+1} \|\boldsymbol{\sigma} \nabla u_h \cdot \mathbf{n}\|_{0,p,\ell}^p &\leq C \left(\|\boldsymbol{\sigma}\|_{1,\infty,T_\ell}^p \|u - u_h\|_{0,p,T_\ell}^p + h_{T_\ell}^{2p} \|[\operatorname{div}(\boldsymbol{\sigma}^I - \boldsymbol{\sigma})] \cdot \nabla u_h\|_{0,p,T_\ell}^p \right. \\ &\quad \left. + |\ell|^{p+1} \|(\boldsymbol{\sigma} - \boldsymbol{\sigma}_\ell) \nabla u_h \cdot \mathbf{n}\|_{0,p,\ell}^p \right), \end{aligned}$$

for all $\ell \in \mathcal{E}_{h,e}$, where $\boldsymbol{\sigma}_\ell$ is any constant matrix.

Proof. We consider an arbitrary $\ell \in \mathcal{E}_{h,e}$, the bubble function b_ℓ defined in (3.8) and

$$\psi_\ell := \boldsymbol{\sigma}_\ell \nabla u_h \cdot \mathbf{n} b_\ell \quad \text{in } \Omega.$$

Like b_ℓ , this function is supported in T_ℓ .

Since $\boldsymbol{\sigma}_\ell$ is constant and b_ℓ satisfies (3.11), it is easy to prove that

$$\begin{aligned}
(4.7) \quad & \|\boldsymbol{\sigma}_\ell \nabla u_h \cdot \mathbf{n}\|_{0,p,\ell}^2 = |\ell|^{2/p-1} \|\boldsymbol{\sigma}_\ell \nabla u_h \cdot \mathbf{n}\|_{0,2,\ell}^2 \\
& \leq C |\ell|^{2/p-1} \|b_\ell^{1/2} \boldsymbol{\sigma}_\ell \nabla u_h \cdot \mathbf{n}\|_{0,2,\ell}^2 \\
& = |\ell|^{2/p-1} \left(\int_\ell (\boldsymbol{\sigma}_\ell - \boldsymbol{\sigma}) \nabla u_h \cdot \mathbf{n} \psi_\ell + \int_\ell \boldsymbol{\sigma} \nabla u_h \cdot \mathbf{n} \psi_\ell \right).
\end{aligned}$$

On the other hand, using that $\|\psi_\ell\|_{0,q,\ell} \leq C |\ell|^{-1/q} \|\psi_\ell\|_{0,q,T_\ell}$ and the arguments used for proving the previous result, we obtain

$$\begin{aligned}
\int_\ell (\boldsymbol{\sigma}_\ell - \boldsymbol{\sigma}) \nabla u_h \cdot \mathbf{n} \psi_\ell & \leq C \|(\boldsymbol{\sigma}_\ell - \boldsymbol{\sigma}) \nabla u_h \cdot \mathbf{n}\|_{0,p,\ell} |\ell|^{-1/q} \|\psi_\ell\|_{0,q,T_\ell} \\
& \leq C \|(\boldsymbol{\sigma}_\ell - \boldsymbol{\sigma}) \nabla u_h \cdot \mathbf{n}\|_{0,p,\ell} |\ell|^{1-2/p} \|\boldsymbol{\sigma}_\ell \nabla u_h \cdot \mathbf{n}\|_{0,p,\ell}
\end{aligned}$$

and

$$\begin{aligned}
\int_\ell \boldsymbol{\sigma} \nabla u_h \cdot \mathbf{n} \psi_\ell & = \int_{T_\ell} (u - u_h) \operatorname{div}(\boldsymbol{\sigma} \nabla \psi_\ell) + \int_{T_\ell} \operatorname{div}(\boldsymbol{\sigma} \nabla u_h) \psi_\ell \\
& \leq C (\|\boldsymbol{\sigma}\|_{1,\infty,T_\ell} \|u - u_h\|_{0,p,T_\ell} |\ell|^{-3/p} \\
& \quad + \|\operatorname{div}(\boldsymbol{\sigma} \nabla u_h)\|_{0,p,T_\ell} |\ell|^{2-3/p}) \|\boldsymbol{\sigma}_\ell \nabla u_h \cdot \mathbf{n}\|_{0,p,\ell}.
\end{aligned}$$

Substituting these expressions in (4.7), we have

$$\begin{aligned}
\|\boldsymbol{\sigma}_\ell \nabla u_h \cdot \mathbf{n}\|_{0,p,\ell} & \leq C |\ell|^{2/p-1} (|\ell|^{-3/p} \|\boldsymbol{\sigma}\|_{1,\infty,T_\ell} \|u - u_h\|_{0,p,T_\ell} \\
& \quad + |\ell|^{2-3/p} \|\operatorname{div}(\boldsymbol{\sigma} \nabla u_h)\|_{0,p,T_\ell} \\
& \quad + |\ell|^{1-2/p} \|(\boldsymbol{\sigma}_\ell - \boldsymbol{\sigma}) \nabla u_h \cdot \mathbf{n}\|_{0,p,\ell})
\end{aligned}$$

and, therefore,

$$\begin{aligned}
|\ell|^{p+1} \|\boldsymbol{\sigma}_\ell \nabla u_h \cdot \mathbf{n}\|_{0,p,\ell}^p & \leq C \left(\|\boldsymbol{\sigma}\|_{1,\infty,T_\ell}^p \|u - u_h\|_{0,p,T_\ell}^p + h_{T_\ell}^{2p} \|\operatorname{div}(\boldsymbol{\sigma} \nabla u_h)\|_{0,p,T_\ell}^p \right. \\
& \quad \left. + |\ell|^{p+1} \|(\boldsymbol{\sigma}_\ell - \boldsymbol{\sigma}) \nabla u_h \cdot \mathbf{n}\|_{0,p,\ell}^p \right).
\end{aligned}$$

Thus, using this result, Lemma 4.2, and the fact that

$$\|\boldsymbol{\sigma} \nabla u_h \cdot \mathbf{n}\|_{0,p,\ell} \leq \|(\boldsymbol{\sigma}_\ell - \boldsymbol{\sigma}) \nabla u_h \cdot \mathbf{n}\|_{0,p,\ell} + \|\boldsymbol{\sigma}_\ell \nabla u_h \cdot \mathbf{n}\|_{0,p,\ell},$$

we conclude the proof. \square

Lemma 4.5. *The following estimate holds true:*

$$h_0^{2-p} \leq C \left(\|\boldsymbol{\sigma}\|_{1,\infty,\omega_{T_0}}^p \|u - u_h\|_{0,p,\omega_{T_0}}^p + \sum_{T' \subset \omega_{T_0}} h_{T'}^{2p} \|[\operatorname{div}(\boldsymbol{\sigma} - \boldsymbol{\sigma}^I)] \cdot \nabla u_h\|_{0,p,T'}^p \right).$$

Proof. Let \mathcal{E}_h^0 be the set of edges ℓ of triangles $T \subset \omega_{T_0}$, such that $\ell \not\subset \partial\omega_{T_0}$. Testing equation (2.3) with the bubble function b_0 defined in (3.14), we obtain

$$\begin{aligned} |\mathbf{p}|^2 &= \mathbf{p} \cdot \nabla b_0(\mathbf{x}_0) = - \int_{\Omega} (u - u_h) \operatorname{div}(\boldsymbol{\sigma} \nabla b_0) - \int_{\Omega} u_h \operatorname{div}(\boldsymbol{\sigma} \nabla b_0) \\ &\leq \|u - u_h\|_{0,p,\omega_{T_0}} \|\operatorname{div}(\boldsymbol{\sigma} \nabla b_0)\|_{0,q,\omega_{T_0}} - \sum_{T' \subset \omega_{T_0}} \int_{T'} \operatorname{div}(\boldsymbol{\sigma} \nabla u_h) b_0 + \sum_{\ell \in \mathcal{E}_h^0} \int_{\ell} [\boldsymbol{\sigma} \nabla u_h]_{\ell} b_0 \\ &\leq C \left(\|u - u_h\|_{0,p,\omega_{T_0}} \|\boldsymbol{\sigma}\|_{1,\infty,\omega_{T_0}} \|b_0\|_{2,q,\omega_{T_0}} \right. \\ &\quad \left. + \|b_0\|_{0,q,\omega_{T_0}} \sum_{T' \subset \omega_{T_0}} \|\operatorname{div}(\boldsymbol{\sigma} \nabla u_h)\|_{0,p,T'} + \sum_{\ell \in \mathcal{E}_h^0} \|[\boldsymbol{\sigma} \nabla u_h \cdot \mathbf{n}]\|_{0,p,\ell} \|b_0\|_{0,q,\ell} \right), \end{aligned}$$

where we have used (3.15), integration by parts, and Hölder inequality.

We estimate $\|b_0\|_{2,q,\omega_{T_0}}$, $\|b_0\|_{0,q,\omega_{T_0}}$, and $\|b_0\|_{0,q,\ell}$ by Corollary 3.4. Thus, we have

$$\begin{aligned} |\mathbf{p}|^2 &\leq Ch_0^{1-2/p} \left(\|\boldsymbol{\sigma}\|_{1,\infty,\omega_{T_0}} \|u - u_h\|_{0,p,\omega_{T_0}} + h_0^2 \sum_{T' \subset \omega_{T_0}} \|\operatorname{div}(\boldsymbol{\sigma} \nabla u_h)\|_{0,p,T'} \right. \\ &\quad \left. + \sum_{\ell \in \mathcal{E}_h^0} |\ell|^{1+1/p} \|[\boldsymbol{\sigma} \nabla u_h \cdot \mathbf{n}]\|_{0,p,\ell} \right). \end{aligned}$$

Since $h_0 \leq Ch_{T'}$ for each $T' \subset \omega_{T_0}$, this estimate together with Lemmas 4.2 and 4.3 lead to the desired result. \square

Now we are in a position to conclude an efficiency estimate by collecting the previous four lemmas. Notice that these lemmas hold true for any $p \in (1, 2)$ (and not only for $p \in (\frac{q_0}{q_0-1}, 2)$) as Theorem 4.1).

Theorem 4.6. *Let $\sigma_{i,j} \in C^1(\overline{\Omega})$ for each $i, j = 1, 2$. Let u and u_h be the solutions of (2.3) and (2.4), respectively. Then, for all $p \in (1, 2)$ and for all $T \in \mathcal{T}_h$*

$$\begin{aligned} \eta_{T,p} &\leq C \left(\|\boldsymbol{\sigma}\|_{1,\infty,\omega_T}^p \|u - u_h\|_{0,p,\omega_T}^p + \sum_{T' \subset \omega_T} h_{T'}^{2p} \|[\operatorname{div}(\boldsymbol{\sigma}^I - \boldsymbol{\sigma})] \cdot \nabla u_h\|_{0,p,T'}^p \right. \\ &\quad \left. + \sum_{\ell \in \mathcal{E}(T) \cap \mathcal{E}_{h,e}} |\ell|^{p+1} \|(\boldsymbol{\sigma} - \boldsymbol{\sigma}_{\ell}) \nabla u_h \cdot \mathbf{n}\|_{0,p,\ell}^p \right)^{1/p}, \end{aligned}$$

where $\omega_T := \{T' \in \mathcal{T}_h : T \cap T' \neq \emptyset\}$, and for each $\ell \in \mathcal{E}(T) \cap \mathcal{E}_{h,e}$, $\boldsymbol{\sigma}_{\ell}$ is any constant matrix.

Notice that the last term in the estimate above vanishes for all triangles which do not intersect $\partial\Omega$.

The above inequalities are actual efficiency estimates if we show that the terms

$$\sum_{T' \subset \omega_T} h_{T'}^{2p} \|[\operatorname{div}(\boldsymbol{\sigma}^I - \boldsymbol{\sigma})] \cdot \nabla u_h\|_{0,p,T'}^p, \quad \sum_{\ell \in \mathcal{E}(T) \cap \mathcal{E}_{h,e}} |\ell|^{p+1} \|(\boldsymbol{\sigma} - \boldsymbol{\sigma}_{\ell}) \nabla u_h \cdot \mathbf{n}\|_{0,p,\ell}^p$$

are negligible. In what follows we will show that this holds true under some additional assumptions; we also note that our final result is true on the whole domain Ω (and not locally, as it would be preferable).

Regarding the term $\sum_{\ell \in \mathcal{E}(T) \cap \mathcal{E}_{h,e}} |\ell|^{p+1} \|(\boldsymbol{\sigma} - \boldsymbol{\sigma}_{\ell}) \nabla u_h \cdot \mathbf{n}\|_{0,p,\ell}^p$, since $\boldsymbol{\sigma}_{\ell}$ is any arbitrary constant matrix, it clearly vanishes when $\boldsymbol{\sigma}|_{\ell}$ is already constant: namely,

when the tissue on the scalp is piecewise homogeneous, which is a realistic assumption in practice. On the other hand, an alternative proof for Lemma 4.4 also holds true when the conductivity on $\partial\Omega$ is of the form $\boldsymbol{\sigma} = \sigma I$, with σ a scalar function; namely, when the tissue of the scalp is isotropic. In fact, in that case we have the following result.

Lemma 4.7. *We have*

$$|\ell|^{p+1} \|\sigma \nabla u_h \cdot \mathbf{n}\|_{0,p,\ell}^p \leq C \left(\|\sigma\|_{1,\infty,T_\ell}^p \|u - u_h\|_{0,p,T_\ell}^p + h_{T_\ell}^{2p} \|[\mathbf{div}(\boldsymbol{\sigma}^I - \boldsymbol{\sigma})] \cdot \nabla u_h\|_{0,p,T_\ell}^p \right)$$

for all $\ell \in \mathcal{E}_{h,e}$, provided $\boldsymbol{\sigma}|_\ell = \sigma I$, with $\sigma : \ell \rightarrow \mathbb{R}$ a scalar function, belonging to $C^1(T_\ell)$.

Proof. We consider an arbitrary $\ell \in \mathcal{E}_{h,e}$, the bubble function b_ℓ defined in (3.8) and

$$\psi_\ell := \sigma_0 \nabla u_h \cdot \mathbf{n} b_\ell \quad \text{in } \Omega,$$

with σ_0 as in (2.2). Like b_ℓ , this function is supported in T_ℓ .

From (3.11) and (2.2), we have that $\int_\ell b_\ell \sigma \geq C \sigma_0 |\ell|$. Using this result, we obtain

$$\begin{aligned} \|\sigma \nabla u_h \cdot \mathbf{n}\|_{0,p,\ell}^2 &\leq \|\sigma\|_{0,\infty,\ell}^2 \|\nabla u_h \cdot \mathbf{n}\|_{0,p,\ell}^2 \\ &= \|\sigma\|_{0,\infty,\ell}^2 |\ell|^{2/p-1} |\ell| \|\nabla u_h \cdot \mathbf{n}\|^2 \\ &\leq C \frac{\|\sigma\|_{0,\infty,\ell}^2}{\sigma_0^2} |\ell|^{2/p-1} \int_\ell \sigma \nabla u_h \cdot \mathbf{n} \psi_\ell. \end{aligned}$$

The rest of the proof runs almost identically as that of Lemma 4.3, by using that

$$\|\psi_\ell\|_{0,q,T_\ell} \leq \|b_\ell\|_{0,q,T_\ell} |\ell|^{-1/p} \|\sigma \nabla u_h \cdot \mathbf{n}\|_{0,p,\ell} \leq C |\ell|^{2-3/p} \|\sigma \nabla u_h \cdot \mathbf{n}\|_{0,p,\ell}$$

and

$$\|\psi_\ell\|_{2,q,T_\ell} \leq C |\ell|^{-2} \|\psi_\ell\|_{0,q,T_\ell} \leq C |\ell|^{-3/p} \|\sigma \nabla u_h \cdot \mathbf{n}\|_{0,p,\ell}$$

instead of (4.5) and (4.6), respectively. \square

In order to prove that the term $\sum_{T' \subset \omega_T} h_{T'}^{2p} \|[\mathbf{div}(\boldsymbol{\sigma}^I - \boldsymbol{\sigma})] \cdot \nabla u_h\|_{0,p,T'}^p$ in Theorem 4.6 is globally negligible, we proceed as in [12] and make the following additional non-degeneracy assumption: there exists $C > 0$ such that

$$(4.8) \quad \|u - u_h\|_{0,p,\Omega} \geq Ch^2.$$

As explained in [12], this assumption looks quite reasonable.

In such a case we conclude with the following result.

Theorem 4.8. *Let us assume that for each $\ell \in \mathcal{E}_{h,e}$, either $\boldsymbol{\sigma}|_\ell$ is a constant matrix, or $\boldsymbol{\sigma}|_\ell = \sigma I$ with $\sigma : \ell \rightarrow \mathbb{R}$ a scalar function. Moreover, we assume that $\boldsymbol{\sigma} \in [C^1(\overline{\Omega})]^{2 \times 2}$ and $\boldsymbol{\sigma} \in [W^{2,\infty}(T)]^{2 \times 2}$ for all $T \in \mathcal{T}_h$. Let u and u_h be the solutions of (2.3) and (2.4), respectively. If (4.8) holds true, then*

$$\eta_p \leq C \|u - u_h\|_{0,p,\Omega}$$

for all $p \in (1, 2)$.

Proof. It is enough to estimate the last term in the inequality of Theorem 4.6:

$$\begin{aligned}
& \sum_{T \in \mathcal{T}_h} \sum_{T' \subset \omega_T} h_{T'}^{2p} \| [\mathbf{div}(\boldsymbol{\sigma}^I - \boldsymbol{\sigma})] \cdot \nabla u_h \|_{0,p,T'}^p \\
& \leq \sum_{T \in \mathcal{T}_h} \sum_{T' \subset \omega_T} h_{T'}^{2p} \| \mathbf{div}(\boldsymbol{\sigma}^I - \boldsymbol{\sigma}) \|_{0,\infty,T'}^p \| \nabla u_h \|_{0,p,T'}^p \\
& \leq C \sum_{T \in \mathcal{T}_h} \sum_{T' \subset \omega_T} h_{T'}^{2p} h_{T'}^p \| \boldsymbol{\sigma} \|_{2,\infty,T'}^p h_{T'}^{-p} \| u_h \|_{0,p,T'}^p \\
& \leq Ch^{2p} (\max_{T \in \mathcal{T}_h} \| \boldsymbol{\sigma} \|_{2,\infty,\omega_T}^p) \sum_{T \in \mathcal{T}_h} \| u_h \|_{0,p,\omega_T}^p \\
& \leq Ch^{2p} (\| u - u_h \|_{0,p,\Omega}^p + \| u \|_{0,p,\Omega}^p) \\
& \leq C \| u - u_h \|_{0,p,\Omega}^p + C \| u - u_h \|_{0,p,\Omega}^p \| u \|_{0,p,\Omega}^p,
\end{aligned}$$

where we have used (4.8) for the last inequality. \square

5. THREE-DIMENSIONAL CASE

In what follows we briefly discuss the results that are preserved in 3D. First, let us recall that the existence and uniqueness of solution of the model problem (2.3) was proved in [16] in the 3D case for all $p \in (1, 3/2)$.

To obtain a priori and a posteriori error estimates for the numerical solution, we resort to the auxiliary problem (2.5). The critical point is the regularity of the solution of this problem. We need that the solution belongs to $W^{2,q}(\Omega)$ for $q > 3$ (namely, q such that $\frac{1}{p} + \frac{1}{q} = 1$ with $1 < p < 3/2$). In [7, Theorem 2] it is proved that if Ω is a cubic domain (namely, a parallelepiped with right angles) and the conductivity σ is a positive constant, (i.e., isotropic homogeneous material), then the solution of (2.5) belongs to $W^{2,q}(\Omega)$ for all $q > 1$. Therefore, within this section we assume that Ω is a cubic domain in \mathbb{R}^3 and that $\boldsymbol{\sigma} = \sigma I$ with σ a positive constant. In such a case we have the following result, that is the analogue in the 3D case of Theorem 2.5.

Theorem 5.1. *Let $\{\mathcal{T}_h\}$ be a quasiuniform family of subdivisions of the cubic domain Ω . Let u and u_h be the solutions to problems (2.3) and (2.4) respectively. Then the following estimate holds true*

$$\| u - u_h \|_{0,p,\Omega} \leq Ch^{3/p-2},$$

for all $p \in (1, 3/2)$.

Proof. The proof runs as that of Theorem 2.5. \square

The a posteriori error analysis also extends to the 3D framework. Let $\mathcal{F}_{h,i}$ be the set of all the inner faces and $\mathcal{F}_{h,e}$ that of external faces of the mesh \mathcal{T}_h . Let $\mathcal{F}_h := \mathcal{F}_{h,i} \cup \mathcal{F}_{h,e}$. For all $T \in \mathcal{T}_h$ we define

$$\begin{aligned}
\widehat{\varepsilon}_{T,p} := & \left(\frac{1}{2} \sum_{F \in \mathcal{F}(T) \cap \mathcal{F}_{h,i}} |F|^{(p+3)/2} |[\nabla u_h \cdot \mathbf{n}_F]|^p \right. \\
& \left. + \sum_{F \in \mathcal{F}(T) \cap \mathcal{F}_{h,e}} |F|^{(p+3)/2} |\nabla u_h \cdot \mathbf{n}_F|^p \right)^{1/p},
\end{aligned}$$

where $\mathcal{F}(T)$ is the set of faces of T and $|F|$ is the area of F .

We define the local a posteriori error indicator $\widehat{\eta}_{T,p}$ for all $T \in \mathcal{T}_h$ by

$$\widehat{\eta}_{T,p} := \begin{cases} \left(h_0^{3-2p} + \widehat{\varepsilon}_{T_0,p}^p \right)^{1/p} & \text{if } T = T_0, \\ \widehat{\varepsilon}_{T,p} & \text{otherwise,} \end{cases}$$

where $h_0 := h_{T_0}$, and the global error estimator from these indicators as follows:

$$\widehat{\eta}_p := \left(\sum_{T \in \mathcal{T}_h} \widehat{\eta}_{T,p}^p \right)^{1/p}.$$

Note that, as we are assuming that σ is constant, the second and third terms that appear in Theorem 4.6 vanish in the estimate of $\widehat{\eta}_{T,p}$. The following results are obtained by adapting to the 3D framework the proofs of Theorem 4.1, and Lemmas 4.3 and 4.5. We have the following result regarding the reliability of the estimator:

Theorem 5.2. *Let u and u_h be the solutions of (2.3) and (2.4), respectively. Then, the following estimate holds true:*

$$\|u - u_h\|_{0,p,\Omega} \leq C \widehat{\eta}_p.$$

The efficiency follows from these two lemmas:

Lemma 5.3. *Let us set $\omega_F := \{T \in \mathcal{T}_h : F \subset \partial T\}$. The following estimates hold true:*

$$|F|^{(p+3)/2} |[\nabla u_h \cdot \mathbf{n}_F]|^p \leq C \|u - u_h\|_{0,p,\omega_F}^p, \quad \text{for all } F \in \mathcal{F}_{h,i}$$

and

$$|F|^{(p+3)/2} |\nabla u_h \cdot \mathbf{n}_F|^p \leq C \|u - u_h\|_{0,p,\omega_F}^p, \quad \text{for all } F \in \mathcal{F}_{h,e}.$$

Lemma 5.4. *Let ω_{T_0} be defined as in (3.13). Then,*

$$h_0^{3-2p} \leq C \|u - u_h\|_{0,p,\omega_{T_0}}^p.$$

Notice that no negligible higher order term appears in this case in the efficiency estimate. Therefore, we have the following version of Theorem 4.8: under the more stringent assumptions we have required, the result now holds locally on each triangle T .

Theorem 5.5. *Let u and u_h be the solutions of (2.3) and (2.4), respectively. Then*

$$\widehat{\eta}_{T,p} \leq C \|u - u_h\|_{0,p,\omega_T},$$

for all $T \in \mathcal{T}_h$ and $p \in (1, 3/2)$.

6. NUMERICAL EXPERIMENTS

In this section we report some numerical experiments in 2D. The adaptive procedure consists in solving problem (2.4) on a sequence of meshes up to finally attain a solution with an estimated error within a prescribed tolerance. Each mesh is a local refinement of the previous one. We compute the local error indicators $\eta_{T,p}$ for all T in the ‘old’ mesh \mathcal{T}_h , and then we refine those elements T with $\eta_{T,p} \geq \theta \max\{\eta_{T,p} : T \in \mathcal{T}_h\}$, where $\theta \in (0, 1)$ is a prescribed parameter. In particular we take $\theta = 1/2$ in all our experiments.

The algorithm is implemented in a Matlab code using the mesh generator Triangle. This generator allows creating successively refined meshes based on a hybrid Delaunay refinement algorithm (see [15]).

6.1. Test 1. Isotropic constant conductivity. The first test consists of solving problem (2.4) in a regular polygon of 16 edges inscribed in a circumference centered at $(0,0)$ with radius 1. The dipole is located at $\mathbf{x}_0 = (0.2605, -0.3054)$, the polarization is $\mathbf{p} = (-0.2425, 0.9701)$ and the conductivity is assumed to be the identity. Since $\sigma = 1$, we can obtain an accurate solution by means of the subtraction technique. This technique uses a particular function u_0 satisfying $\operatorname{div}(\sigma \nabla u_0) = \operatorname{div}(\mathbf{p} \delta_{\mathbf{x}_0})$, which is analytically known. Subtracting u_0 to the solution of problem (2.4) leads to a non-homogeneous Neumann problem, whose solution is not singular at \mathbf{x}_0 . Therefore, this problem can be accurately solved by using standard finite elements (see [18] for more details). The solution computed by this subtraction technique in the finest mesh of the adaptive procedure will be taken as the reference solution, $u_{\text{ref}}(\mathbf{x})$.

Figure 5 shows some of the successively refined meshes created in the process driven by $\eta_{T,p}$ with $p = 1.25$. Parameters “iter” and “d.o.f.” refer to the iteration number and the total number of vertices of the corresponding mesh.

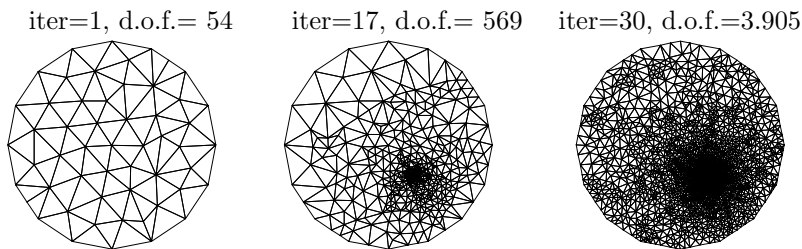


FIGURE 5. Test 1. Meshes obtained with $\eta_{T,p}$; $p = 1.25$.

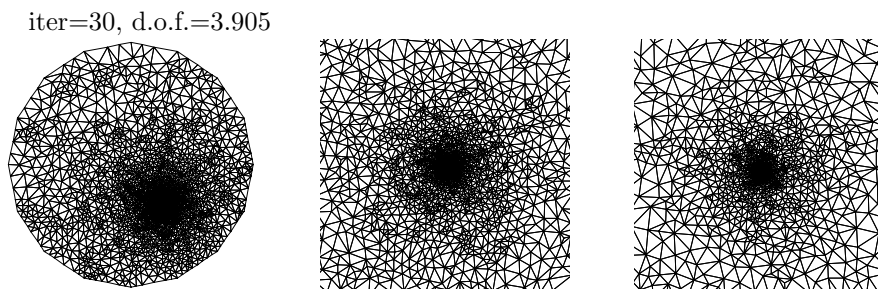


FIGURE 6. Test 1. Zooms of the mesh for iter=30.

Figure 6 shows two successive zooms around the singularity of the finer mesh in Figure 5. Each figure is a 200% zoom of the previous one. It can be appreciated that the mesh is extremely refined in the neighborhood of the singular point. Such a behavior can be expected from the singularity of the solution at \mathbf{x}_0 , which can be seen from Figure 7, which shows the computed solution on some of the coarser meshes. (Notice that the vertical scales are different on each subfigure.)

This extremely singular behavior is the reason why the adaptively created meshes are so localized. This can be appreciated in Figure 8, which contains two graphs. The one on the left shows the plot of the discrete solution corresponding to the

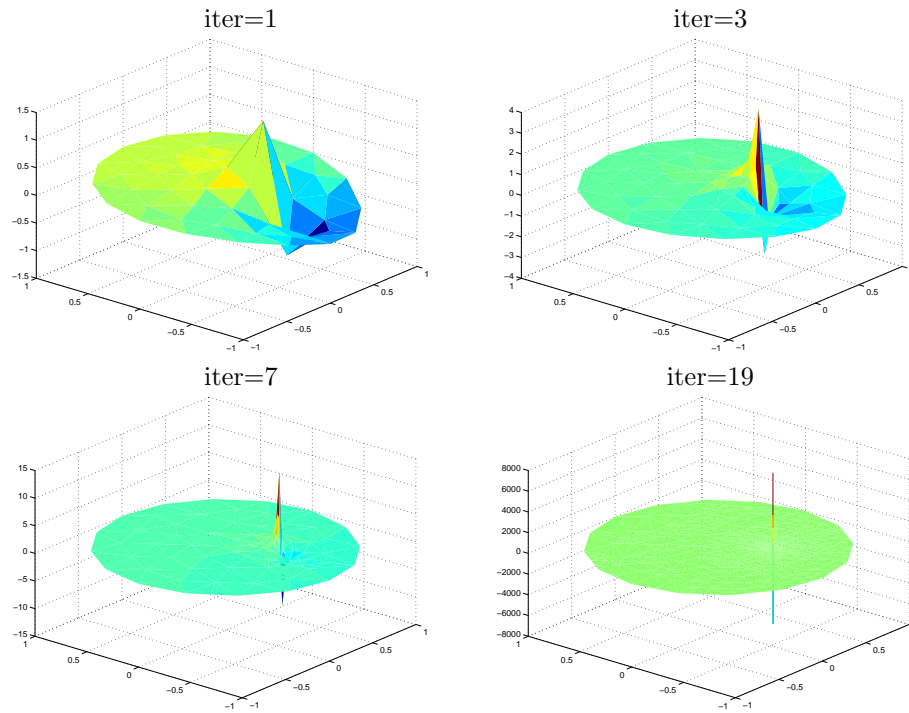
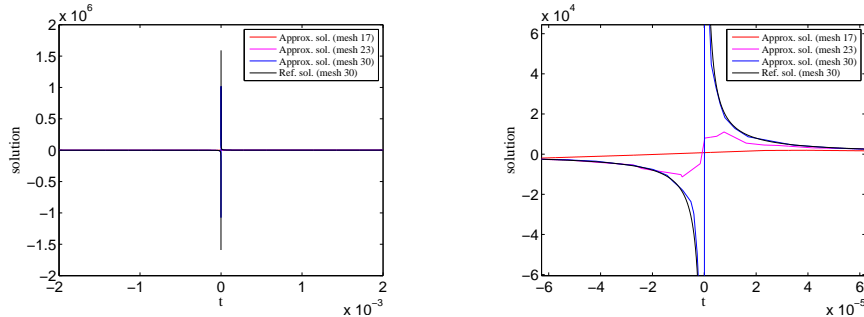


FIGURE 7. Test 1. Approximate solutions on some coarser meshes.

different meshes on the segment $\mathbf{x} = \mathbf{x}_0 + t\mathbf{p}$, $t \in [-0.002, 0.002]$. The right subfigure is a zoom of previous the plot.

FIGURE 8. Test 1. Approximate solution and exact solution on the segment $\mathbf{x} = \mathbf{x}_0 + t\mathbf{p}$, $t \in [-0.002, 0.002]$.

The behavior of the (absolute) error along the adaptive process can be seen from Figure 9. We report log-log plots of the estimated error and the “reference error” versus the number of degrees of freedom. The “reference error” is computed by comparing the solution of problem (2.4) with the reference solution. The figure also shows a line of slope -1 which corresponds to the optimal order of convergence

	Degrees of freedom	L^p relative error
Adapted mesh 9	141	$0.4368 \cdot 10^{-1}$
Adapted mesh 32	5794	$0.1152 \cdot 10^{-2}$
Quasiuniform mesh	5780	$0.5508 \cdot 10^{-1}$

TABLE 1. Test 1. The L^p relative error for $p = 1.25$ in three different meshes

for the finite elements used. It can be seen that the estimated and the reference errors both attain this optimal order.

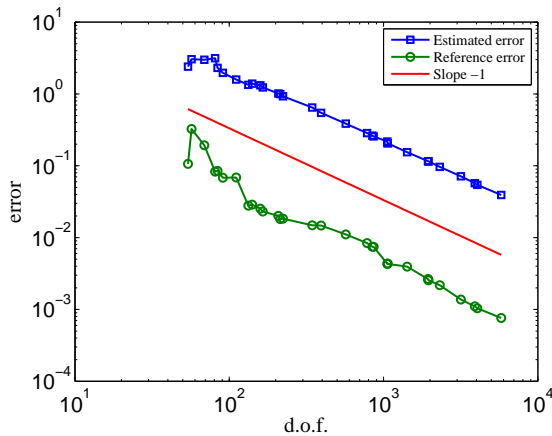


FIGURE 9. Test 1. Estimator η_p and reference (absolute) L^p error curves; $p = 1.25$.

In Table 1 we compare the reference (relative) error for the solution of problem (2.4) computed using adapted meshes and a quasiuniform mesh with approximately the same number of nodes (5780). It can be seen that, to obtain a solution with an error around 5 %, the number of d.o.f. in the uniform mesh is 40 times the number of d.o.f. in the adapted mesh. Moreover, with almost the same number of d.o.f., the adaptive algorithm yields a computed solution with an error 50 times smaller than the one obtained with a uniform mesh.

We notice also that, though the error indicator is designed to estimate the L^p -norm in Ω , when using this adaptive procedure the error on the boundary decreases at the optimal rate, too. Thus, this error indicator can be used in the forward solver when facing the inverse problem of electroencephalography (namely, the problem aiming at determining the source localization from suitable boundary measurements). In Figure 10 we present a log-log plot of the averaged relative error $\sqrt{\sum_{n=1}^{12} |(u_h - u_{\text{ref}})(\mathbf{x}_n)|^2 / \sum_{n=1}^{12} |u_{\text{ref}}(\mathbf{x}_n)|^2}$ in twelve different points of $\partial\Omega$ (twelve consecutive vertexes of the polygon Ω), which can be thought as the localization of the electrodes. Although this error is more noisy, a fated optimal order (slope -1) can be appreciated.

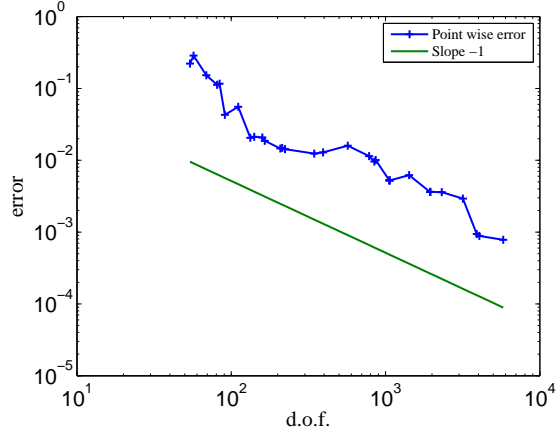
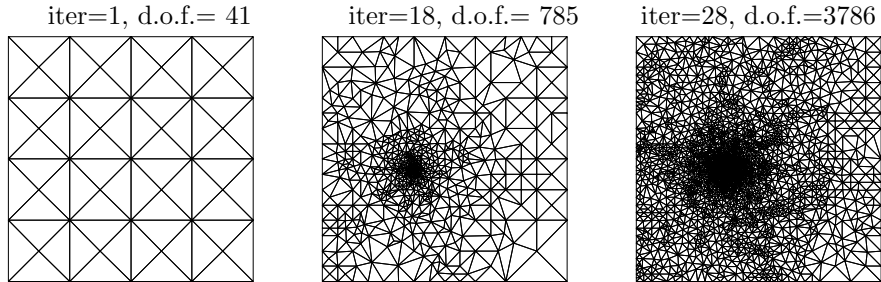


FIGURE 10. Test 1. Averaged relative error at boundary points.

6.2. Test 2. Anisotropic non-constant conductivity. In the second test, Ω is a square centered at $(0, 0)$ with side-length 2. The dipole is located at $\mathbf{x}_0 = (-0.25000, -0.08333)$, and the polarization is $\mathbf{p} = (0.9015, 0.4327)$. We consider a non-constant anisotropic conductivity

$$\boldsymbol{\sigma} = \begin{pmatrix} 4x^2 + 1 & 0 \\ 0 & 2y^2 + 1 \end{pmatrix}.$$

The results are very similar to those of the previous example. Figure 11 contains the meshes corresponding to three different iterations of the adaptive scheme and Figure 12 shows two successive zooms around the singularity.

FIGURE 11. Test 2. Meshes obtained with $\eta_{T,p}$; $p = 1.25$.

We report in Figure 13 a log-log plot of the estimated error versus the number of degrees of freedom. The slope is close to -1 which confirms the success of the approach. In this case we have not a reference solution because the subtracting approach can not be used in this case, since the conductivity is not constant around the point where the source is located.

6.3. Test 3. Anisotropic constant conductivity. Finally, we consider a strongly anisotropic conductivity: $\boldsymbol{\sigma} = \begin{pmatrix} 10 & 0 \\ 0 & 0.1 \end{pmatrix}$. The domain Ω is a square centered at

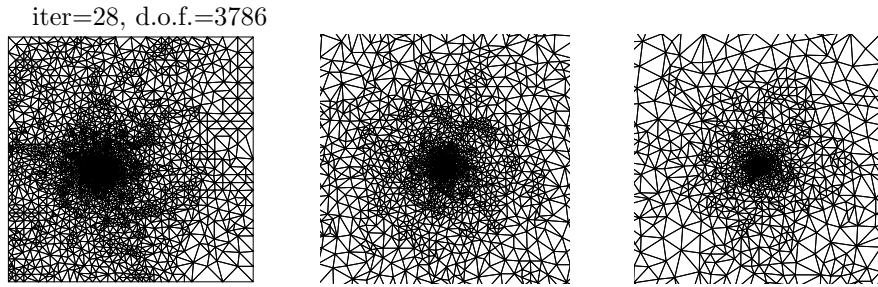


FIGURE 12. Test 2. Zooms of the mesh for iter=28.

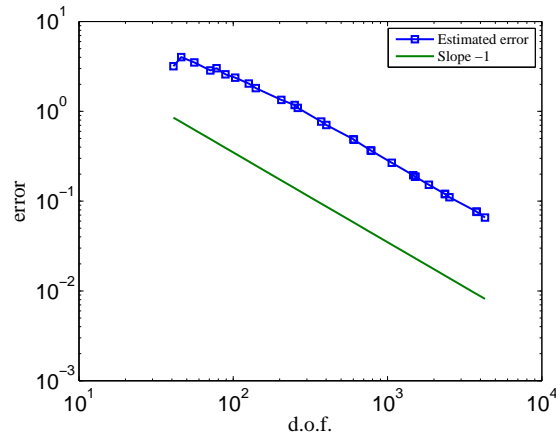


FIGURE 13. Test 2. Estimator η_p curve; $p = 1.25$.

$(0, 0)$, with side-length 2. The dipole is located at $\mathbf{x}_0 = (0, 0)$ and the polarization is $\mathbf{p} = (1, 1)$. Since the conductivity is constant, as in the first test we can compute the reference solution using the subtraction approach.

We show in Figure 14 the meshes corresponding to three different iterations of the adaptive scheme. Figure 15 shows two successive zooms around the singularity of the finest mesh considered (iter=45, d.o.f.=4168).

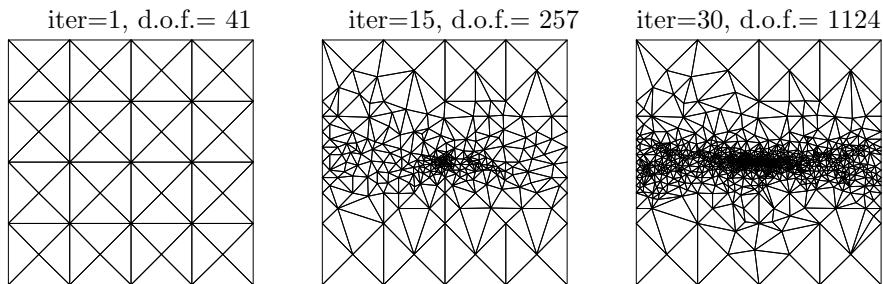


FIGURE 14. Test 3. Meshes obtained with $\eta_{T,p}$; $p = 1.25$.

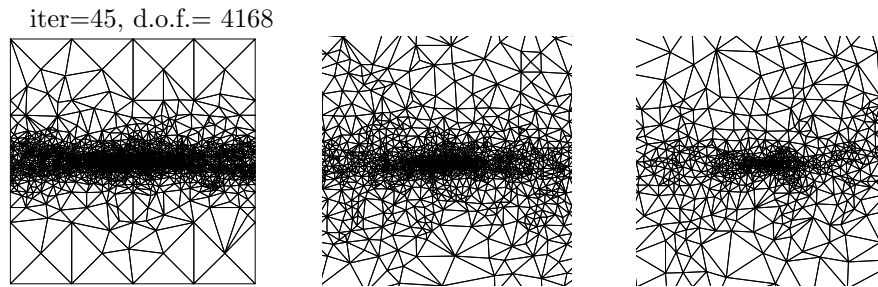


FIGURE 15. Test 3. Zooms of the mesh around the singular point for iter=45.

It can be clearly seen that in this case the meshes are not only refined around the singular point. The reason for this is that, because of the anisotropy of the conductivity, the solution has an inner layer at $x_2 = 0$. In fact, the fundamental solution (which is the only source of singularity) reads in this case

$$u_0(\mathbf{x}) = \frac{1}{2\pi} \frac{x_1 + 100x_2}{x_1^2 + 100x_2^2}.$$

Therefore, it is easy to check that the slope of the graph in the x_2 -direction is approximately $\frac{100}{x_1^2}$ at $x_2 = 0$. This can be seen from Figure 16, which shows the plot of the fundamental solution in a uniform mesh with 8321 vertices.

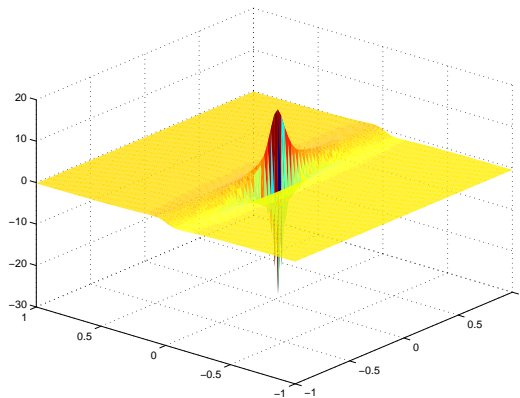


FIGURE 16. Test 3. Fundamental solution.

We notice from Figure 17 that the computed order of convergence is not optimal in this example. In fact, the fitted slope is close to -0.57 . Very likely, the reason for this suboptimal order is that our adaptive scheme only uses regular meshes, while appropriate anisotropic meshes seem to be necessary around the inner layer. Nevertheless, the use of our adaptive procedure turns out to be convenient, as can be seen by comparison with the results obtained with uniform refinement (see Table 2).

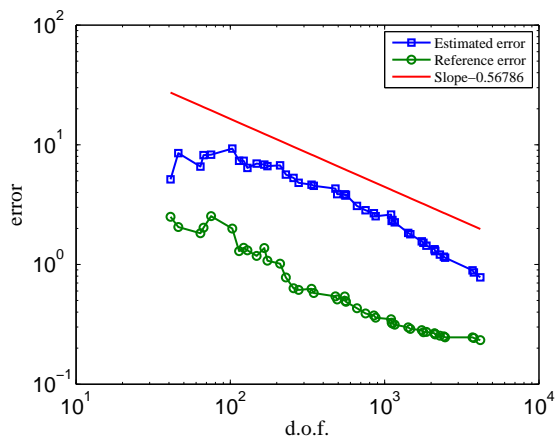


FIGURE 17. Test 3. L^p (absolute) error curves for $p = 1.25$: estimated and reference error on adapted meshes.

	Degrees of freedom	L^p relative error
Adapted mesh 15	257	$0.7217 \cdot 10^{-1}$
Adapted mesh 38	2118	$0.3007 \cdot 10^{-1}$
Quasiuniform mesh	2113	$0.7417 \cdot 10^{-1}$

TABLE 2. Test 3. The L^p relative error for $p = 1.25$ in three different meshes.

REFERENCES

- [1] R. ARAYA, E. BEHRENS, AND R. RODRÍGUEZ, *A posteriori error estimates for elliptic problems with Dirac delta source terms*, Numer. Math., 105 (2006), pp. 193–216.
- [2] K. AWADA, D. JACKSON, J. WILLIAMS, D. WILTON, S. BAUMANN, AND A. PAPANICOLAOU, *Computational aspects of finite element modeling in EEG source localization*, IEEE Trans. Biomed. Eng., 44 (1197), pp. 736–752.
- [3] S. C. BRENNER AND L. R. SCOTT, *The Mathematical Theory of Finite Element Methods*, Springer, New York, third ed., 2008.
- [4] H. BUCHNER, G. KNOLL, M. FUCHS, A. RIENÄCKER, R. BECKMANN, M. WAGNER, J. SILNY, AND J. PESCH, *Inverse localization of electric dipole current sources in finite element models of the human head*, Electroenc. Clin. Neurophysiol., 102 (1997), pp. 267–278.
- [5] P. G. CIARLET, *The Finite Element Method for Elliptic Problems*, North-Holland, Amsterdam, 1978.
- [6] P. G. CIARLET, *Basic error estimates for elliptic problems*, in Handbook of Numerical Analysis, Vol. II, P. G. Ciarlet and J.-L. Lions, eds., North-Holland, Amsterdam, 1991, pp. 17–351.
- [7] M. DAUGE, *Problèmes de Neumann et de Dirichlet sur un polyèdre dans \mathbf{R}^3 : régularité dans des espaces de Sobolev L_p* , C. R. Acad. Sci. Paris Sér. I Math., 307 (1988), pp. 27–32.
- [8] ———, *Neumann and mixed problems on curvilinear polyhedra*, Integral Equations Operator Theory, 15 (1992), pp. 227–261.
- [9] M. HÄMÄLÄINEN, R. HARI, R. J. ILMONIEMI, J. KNUUTILA, AND O. V. LOUNASMAA, *Magnetoencephalography – theory, instrumentation, and applications to noninvasive studies of the working human brain*, Rev. Mod. Phys., 65 (1993), pp. 413–497.
- [10] S. LEW, C. H. WOLTERS, T. DIERKES, C. RÖER, AND R. S. MACLEOD, *Accuracy and runtime comparison for differential potential approaches and iterative solvers in finite element method based EEG source analysis*, Appl. Numer. Math., 59 (2009), pp. 1970–1988.

- [11] J. C. MOSHER, R. M. LEAHY, AND P. S. LEWIS, *EEG and MEG: forward solutions for inverse methods*, IEEE Trans. Biomed. Engrg., 46 (1999), pp. 245–259.
- [12] R. H. NOCHETTO, *Pointwise a posteriori error estimates for elliptic problems on highly graded meshes*, Math. Comp., 64 (1995), pp. 1–22.
- [13] J. SARVAS, *Basic mathematical and electromagnetic concepts of the biomagnetic inverse problem*, Phys. Med. Biol., 32 (1987), pp. 11–22.
- [14] P. SCHIMPF, C. RAMON, AND H. J. HAUEISEN, *Dipole models for the EEG and MEG*, IEEE Trans. Biomed. Eng., 49 (2002), pp. 409–418.
- [15] J. R. SHEWCHUK, *Delaunay refinement algorithms for triangular mesh generation*, Comput. Geom., 22 (2002), pp. 21–74.
- [16] A. VALLI, *Solving an electrostatics-like problem with a current dipole source by means of the duality method*, Appl. Math. Lett., 25 (2012), pp. 1410–1414.
- [17] D. WEINSTEIN, L. ZHUKOV, AND C. JOHNSON, *Lead-field bases for electroencephalography source imaging*, Ann. of Biomed. Eng., 28 (2000), pp. 1059–1066.
- [18] C. H. WOLTERS, H. KÖSTLER, C. MÖLLER, J. HÄRDITLEIN, L. GRASEDYCK, AND W. HACKBUSCH, *Numerical mathematics of the subtraction method for the modeling of a current dipole in EEG source reconstruction using finite element head models*, SIAM J. Sci. Comput., 30 (2007/08), pp. 24–45.
- [19] Y. YAN, P. NUNEZ, AND R. HART, *Finite-element model of the human head: Scalp potentials due to dipole sources*, Med. Biol. Eng. Comput., 29 (1991), pp. 475–481.

DEPARTMENT OF MATHEMATICS, UNIVERSITY OF TRENTO, VIA SOMMARIVE 14, 38123 POVO (TRENTO), ITALY.

E-mail address: `alonso@science.unitn.it`

CI²MA, DEPARTAMENTO DE INGENIERÍA MATEMÁTICA, UNIVERSIDAD DE CONCEPCIÓN, CASILLA 160-C, CONCEPCIÓN, CHILE.

E-mail address: `jcamano@ing-mat.udec.cl`

CI²MA, DEPARTAMENTO DE INGENIERÍA MATEMÁTICA, UNIVERSIDAD DE CONCEPCIÓN, CASILLA 160-C, CONCEPCIÓN, CHILE.

E-mail address: `rodolfo@ing-mat.udec.cl`

DEPARTMENT OF MATHEMATICS, UNIVERSITY OF TRENTO, VIA SOMMARIVE 14, 38123 POVO (TRENTO), ITALY.

E-mail address: `valli@science.unitn.it`

Centro de Investigación en Ingeniería Matemática (CI²MA)

PRE-PUBLICACIONES 2012 - 2013

- 2012-25 RAIMUND BÜRGER, PEP MULET, LUIS M. VILLADA: *A diffusively corrected multi-class Lighthill-Whitham-Richards traffic model with anticipation lengths and reaction times*
- 2012-26 MARGARETH ALVES, JAIME MUÑOZ-RIVERA, MAURICIO SEPÚLVEDA, OCTAVIO VERA: *Exponential and the lack of exponential stability in transmission problems with localized Kelvin-Voigt dissipation*
- 2013-01 JORGE CLARKE, CIPRIAN A. TUDOR: *Wiener integrals with respect to the Hermite random field and applications to the wave equation*
- 2013-02 JULIO ARACENA, ADRIEN RICHARD, LILIAN SALINAS: *Maximum number of fixed points in AND-OR Boolean network*
- 2013-03 RAIMUND BÜRGER, RICARDO RUIZ-BAIER, CANRONG TIAN: *Stability analysis and finite volume element discretization for delay-driven spatial patterns in a predator-prey model*
- 2013-04 TOMÁS BARRIOS, ROMMEL BUSTINZA, GALINA C. GARCÍA, MARÍA GONZÁLEZ: *A posteriori error analyses of a velocity-pseudostress formulation of the generalized Stokes problem*
- 2013-05 RODOLFO ARAYA, ABNER POZA, FREDERIC VALENTIN: *An adaptive residual local projection finite element method for the Navier-Stokes equations*
- 2013-06 MOHAMED HELAL, ERWAN HINGANT, LAURENT PUJO-MENJOUET, GLENN WEBB: *Alzheimer's disease: Analysis of a mathematical model incorporating the role of prions*
- 2013-07 RICARDO OYARZÚA, DOMINIK SCHÖTZAU: *An exactly divergence-free finite element method for a generalized Boussinesq problem*
- 2013-08 HERNÁN MARDONES, CARLOS M. MORA: *Stable numerical methods for two classes of SDEs with multiplicative noise: bilinear and scalar*
- 2013-09 ALFREDO BERMÚDEZ, DOLORES GÓMEZ, RODOLFO RODRÍGUEZ, PABLO VENEGAS: *Mathematical and numerical analysis of a transient non-linear axisymmetric eddy current model*
- 2013-10 ANA ALONSO-RODRIGUEZ, JESSIKA CAMAÑO, RODOLFO RODRÍGUEZ, ALBERTO VALLI: *A posteriori error estimates for the problem of electrostatics with a dipole source*

Para obtener copias de las Pre-Publicaciones, escribir o llamar a: DIRECTOR, CENTRO DE INVESTIGACIÓN EN INGENIERÍA MATEMÁTICA, UNIVERSIDAD DE CONCEPCIÓN, CASILLA 160-C, CONCEPCIÓN, CHILE, TEL.: 41-2661324, o bien, visitar la página web del centro: <http://www.ci2ma.udec.cl>



**CENTRO DE INVESTIGACIÓN EN
INGENIERÍA MATEMÁTICA (CI²MA)
Universidad de Concepción**



Casilla 160-C, Concepción, Chile
Tel.: 56-41-2661324/2661554/2661316
<http://www.ci2ma.udec.cl>